JOURNAL OF COMPUTATIONAL PHYSICS 10, 568–606 (1972)

Sixth-Order Effects in Nucleon–Nucleon Scattering*

J. L. GAMMEL AND W. R. WORTMAN†

Los Alamos Scientific Laboratory, University of California
Los Alamos, New Mexico 87544

Received October 4, 1971

Some of the series resulting from quantum field theory are known to be summable by Padé approximants. As a test of the feasibility of generating such series by numerically calculating the Feynman graphs in each order, we have calculated sixth order graphs for nucleon–nucleon scattering with pseudoscalar pion exchange. Graphs with a $\lambda\varphi^4$ interaction of the pions are also calculated. We find that a modification of the Monte Carlo technique is essential to obtain accuracy, and that certain variable transformations are necessary to eliminate integrable boundary singularities which remain after renormalization. A brief discussion of the physical significance of the magnitude of the sixth-order terms is included.

I. INTRODUCTION

Padé approximants have been useful in summing the series arising in statistical physics [1] and in obtaining useful information concerning, for example, the nature of the singularity at the Curie temperature predicted by the Ising and Heisenberg models. It is not definitely known that the series resulting from quantum field theory are similarly summable, although much progress has been made in closely analogous problems [3] or even problems of more obvious relevance [4].

What one would like to do is calculate the perturbation series for (say) nucleon–nucleon scattering to high order and form the Padé approximants to test whether or not they converge. In statistical physics, such a test was possible a long time ago because the formidable task of calculating the series was completed before the use of the Padé approximant was common in physics [1]. In quantum field theory, some calculations of pion–pion scattering have proceeded through a sufficiently high order so that at least the first two Padé approximants in what should be an infinite sequence can be formed [5]. For nucleon–nucleon scattering, only the first has been calculated [6], but due to anomalous threshold dependences

* Work performed under the auspices of the U. S. Atomic Energy Commission.

† Present address: Service de Physique Théorique, CEN-Saclay, B. P. No. 2, GIF-sur-YVETTE, France.

of some of the amplitudes, not much could be expected of the first Padé approximant anyhow.

We are led, therefore, to study the feasibility of higher order calculations in the nucleon–nucleon problem. Since it has been found that a $\lambda\varphi^4$ interaction can reproduce the ρ-resonance [7], this interaction will be included with the usual $\overline{\Psi}\gamma_5\Psi\varphi$ interaction. The ρ is commonly used in one boson exchange models. The graphs arising from the $\lambda\varphi^4$ interaction which are made finite by renormalization have integrable singularities (remnants of their divergent character before renormalization) on the boundaries of the region over which the Feynman variables are integrated. One purpose of the work is to study how these integrable singularities are best handled.

The magnitudes of the sixth-order terms are of some interest for more conventional views of the utility of quantum field theory (the view that the series must converge to be useful). This view is that the series might be useful for higher angular momenta, or might be useful if various partial summations or certain types of graphs were effected somehow. We comment briefly on the results from this more conventional point of view in Section V, but we wish to emphasize that our own is quite different and that our purpose in the present work is to establish techniques and feasibility rather than to obtain specific results.

It is to be hoped that someday it will be possible to do the tedious Dirac algebra and the other algebra involved in these calculations on computing machines [8]. Our results should provide useful checks of automated calculations, and we expect that such checks are the most valuable aspect of the present work.

II. Methods

A. *Preliminary considerations*

The interaction for this calculation is taken as

$$\mathscr{H}_I = i(4\pi)^{1/2} g\overline{\Psi}\gamma_5\tau\Psi \cdot \boldsymbol{\varphi} + 4\pi\lambda(\boldsymbol{\varphi} \cdot \boldsymbol{\varphi})^2, \tag{1}$$

where the Dirac equation is $(i\gamma \cdot p + m)\, u(p) = 0$. The conventions used are $\hbar = c = 1$, $g^2 \simeq 14$, $\bar{u}u = 1$, $\gamma_\mu\gamma_\nu + \gamma_\nu\gamma_\mu = 2\delta_{\mu\nu}$, and $\gamma_5{}^2 = 1$. The resulting set of graphs to be considered is shown in Fig. 1. Graphs which require the usual vertex and self-energy renormalization have been ignored on the strength of a fourth-order calculation which indicates that they are small [13].

The graphs have such diverse characteristics that it is found that a variety of methods is required to evaluate them. However, with the exception of the ladder graph (Fig. 1(e)), the basic method is the same. We express the amplitudes first in the usual form as integrals over the internal momenta and then convert these

to multiple integrals over Feynman parameters using Chisholm's methods [14]. These methods provide the usual means of combining denominators and trading the momenta integrals for integrals over Feynman parameters while dealing with the spin complications in a straightforward way.

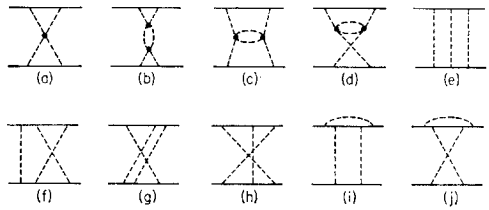

FIG. 1. Perturbation theory graphs which will be considered.

The chief difficulties resulting from this procedure are the need for reducing the resulting spinors to combinations of the standard five NN amplitudes and the necessity of carrying out resulting multiple integrals, some of which contain singular integrands. The second difficulty is the more serious.

B. *Chisholm method*

The Chisholm method [14] is carried out by writing the nucleon propagators as

$$\frac{i}{(2\pi)^4}\frac{i\gamma\cdot(p+k)-m}{(p+k)^2+m^2}=\frac{i}{(2\pi)^4}\left[-m-\frac{i\gamma}{2}\cdot\frac{\partial}{\partial p}\int_{m^2}^{\infty}d\sigma\right]\frac{1}{(p+k)^2+\sigma}$$
$$\equiv\frac{i}{(2\pi)^4}F(p,m)\frac{1}{(p+k)^2+\sigma}. \tag{2}$$

Here σ is to be set to the proper m^2 after the operation denoted by F is performed. Thus the amplitude becomes that of the corresponding scalar case except for the operations F that remain to be carried out.

The propagators for the internal lines can be combined in the usual way by noting that

$$[a_1a_2\cdots a_{n+1}]^{-1}$$
$$=n!\int_0^1 dx_1\int_0^{x_1}dx_2\cdots\int_0^{x_{n-1}}dx_n$$
$$\times[a_1(1-x_1)+a_2(x_1-x_2)+\cdots+a_n(x_{n-1}-x_n)+a_{n+1}x_n]^{-(n+1)}. \tag{3}$$

Therefore the integrals are reduced to the form

$$\int dx_i\int d^4k_1\cdots d^4k_l[Q(k_1,\ldots,k_l,x_i)]^{-r}, \tag{4}$$

where l is the number of internal momenta and r is the number of internal lines in the graph. The quantity Q is at most quadratic in the momenta and can be written [omitting dots which indicate scalar products in Eqs. (5)–(9)]

$$Q = \Sigma A_{ij} k_i k_j + 2\Sigma B_i k_i + C. \tag{5}$$

By an appropriate orthogonal transformation and translation in $k_1 \cdots k_l$ space, Q can be transformed to

$$Q' = \Sigma A_i' k_i'^2 + C'. \tag{6}$$

The momenta integrals can be explicitly evaluated, giving

$$\int d^4k_i [Q(k_1 \cdots k_l, x_i)]^{-r} = (i\pi^2)^l \frac{(r-2l-1)!}{(r-1)!} \frac{\Lambda^{r-2l-2}}{\chi^{r-2l}}. \tag{7}$$

Here Λ and χ are the determinants

$$\Lambda = \begin{vmatrix} A_{11} & A_{12} & \cdots & A_{1l} \\ A_{21} & A_{22} & \cdots & A_{2l} \\ \vdots & \vdots & & \vdots \\ A_{l1} & A_{l2} & \cdots & A_{ll} \end{vmatrix}, \tag{8}$$

and

$$\chi = \begin{vmatrix} A_{11} & A_{12} & \cdots & A_{1l} & B_1 \\ \vdots & \vdots & & \vdots & \vdots \\ A_{l1} & A_{l2} & \cdots & A_{ll} & B_l \\ B_1 & B_2 & \cdots & B_l & C \end{vmatrix}. \tag{9}$$

Now Λ is independent of the external momenta p so that the F operators will affect only χ. Chisholm [14] has investigated the result of a series of F's operating on χ^{-r} and the result is conveniently expressed in terms of quantities Ω_i and Ω_{ij}. If one assigns a momentum $P^i + K_i$ to the i-th internal line, then P^i will be some linear combination of the external momenta, perhaps zero, and K_i will be some linear combination of the internal momenta k_j. If P^i for some nucleon line is zero, then a fictitious P^i is assigned to be set to zero after the F operations are performed. The coefficient of $(P^i + K_i)^2 + \sigma_i$ in Q will be denoted by C_i. Finally defining ∂_{ij} as the coefficient of k_j in K_i, which may be ± 1, or 0, Ω_{ij} is

$$\Omega_{ij} = \frac{1}{2\Lambda^2} \begin{vmatrix} A_{11} & A_{12} & \cdots & A_{1l} & \partial_{il} \\ A_{21} & A_{22} & \cdots & A_{2l} & \partial_{i2} \\ \vdots & \vdots & & \vdots & \vdots \\ A_{l1} & A_{l2} & \cdots & A_{ll} & \partial_{il} \\ \partial_{j1} & \partial_{j2} & \cdots & \partial_{jl} & \delta_{ij}/C_i \end{vmatrix}, \tag{10}$$

and

$$\Omega_i + m = 2\Lambda \sum_j \Omega_{ij} C_j i\gamma \cdot P^j. \tag{11}$$

Prior to carrying out the F operations, the numerator will be some combination of F's and γ matrices such as

$$\bar{u}_1\gamma_5 F_1\gamma_5 F_2\gamma_5 u_1\bar{u}_2\gamma_5 F_3\gamma_5 F_4\gamma_5 u_2[\chi^{-r}]. \tag{12}$$

The result of the F_i operations is a "basic term"

$$\bar{u}_1\gamma_5\Omega_1\gamma_5\Omega_2\gamma_5 u_1\bar{u}_2\gamma_5\Omega_3\gamma_5\Omega_4\gamma_5 u_2[\chi^{-r}], \tag{13}$$

plus terms found by substituting γ_μ for all possible pairs of Ω_i while noting the effect of the derivative in F. This gives, for example,

$$\bar{u}_1\gamma_5\gamma_\mu\gamma_5\gamma_\mu\gamma_5 u_1\bar{u}_2\gamma_5\Omega_3\gamma_5\Omega_4\gamma_5 u_2\Omega_{12}[\chi^{-(r-1)}/(r-1)]. \tag{14}$$

There will be six such terms. Additional terms are found by substituting two pairs of γ_μ's for the Ω_i which gives, for example,

$$\bar{u}_1\gamma_5\gamma_\mu\gamma_5\gamma_\mu\gamma_5 u_1\bar{u}_2\gamma_5\gamma_\nu\gamma_5\gamma_\nu\gamma_5 u_2\Omega_{12}\Omega_{34}[\chi^{-(r-2)}/(r-2)(r-1)]. \tag{15}$$

There will be three such terms.

By this procedure one obtains a numerator which is a sum of terms which are combinations of spinors, γ-matrices, and Feynman parameters. This must be written as combinations of the five NN scattering amplitudes as

$$\begin{aligned} F = {} & A_1[\bar{u}_1 u_1\bar{u}_2 u_2] \\ & + A_2[\bar{u}_1 u_1\bar{u}_2 i\gamma \cdot p_1 u_2 + \bar{u}_1 i\gamma \cdot p_2 u_1\bar{u}_2 u_2] \\ & + A_3[\bar{u}_1 i\gamma \cdot p_2 u_1\bar{u}_2 i\gamma \cdot p_1 u_2] \\ & + A_4[\bar{u}_1\gamma_\mu u_1\bar{u}_2\gamma_\mu u_2] \\ & + A_5[\bar{u}_1\gamma_5 u_1\bar{u}_2\gamma_5 u_2]. \end{aligned} \tag{16}$$

The external momenta are labeled as shown in Fig. 2 and the spinors have the arguments $\bar{u}_1(p_1')$, $u_1(p_1)$, $\bar{u}_2(p_2')$, and $u_2(p_2)$.

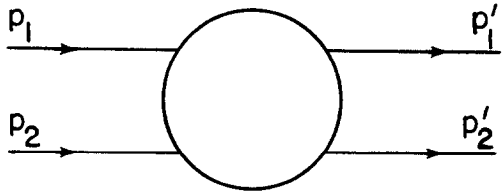

FIG. 2. Definition of external momenta.

In general, other combinations of spinors will occur but they can always be reduced to the form of (16) plus other terms whose coefficients will vanish due to time-reversal invariance (TRI). This last condition serves as a useful check on the calculation.

C. *Example calculation*

As an example of this procedure consider the graph of Fig. 3. The choice of momenta k_1 and k_2 is somewhat arbitrary and the associated combinations of the external momenta P^i are given in Table I. In terms of the contribution to the S-matrix, the invariant amplitude F is

$$S = 1 + i(2\pi)^4 \delta(\Sigma p_i - \Sigma p_f) N_1 N_2 N_3 N_4 F, \tag{17}$$

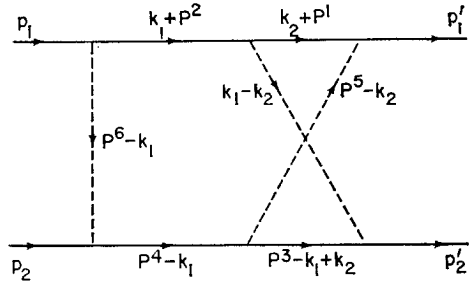

FIG. 3. A sixth-order graph.

TABLE I

Parameters associated with the graph in the example calculation

i	1	2	3	4	5	6
C_i	$1 - x_1$	x_6	$x_2 - x_3$	$x_5 - x_6$	$x_1 - x_2$	$x_4 - x_5$
∂_{i1}	0	1	−1	−1	0	−1
∂_{i2}	1	0	1	0	−1	0
P^i	0	0	p_2'	$p_1 + p_2$	p_1'	p_1

where $N_i = ((1/(2\pi)^3)\, m_i/E_i)^{1/2}$. Therefore for the graph of Fig. 3,

$$\begin{aligned} F = {} & (g^2)^3 (4\pi^5)^{-1} \int d^4k_1 d^4k_2 \bar{u}_1 \gamma_5 [i\gamma \cdot k_2 - m] \\ & \times \gamma_5 [i\gamma \cdot k_1 - m]\, \gamma_5 u_1 ([k_2^2 + m^2][k_1^2 + m^2])^{-1} \\ & \times \frac{\bar{u}_2 \gamma_5 [i\gamma \cdot (p_2' + k_2 - k_1) - m]\, \gamma_5 [i\gamma \cdot (p_1 + p_2 - k_1) - m]\, \gamma_5 u_2}{\left[\begin{array}{r}(p_1' - k_2)^2 + \mu^2][(p_2' - k_1 + k_2)^2 + m^2][(k_1 - k_2)^2 + \mu^2] \\ [(p_1 - k_1)^2 + \mu^2][(p_1 + p_2 - k_1)^2 + m^2]\end{array}\right]}. \end{aligned} \tag{18}$$

Combining the denominators as in (3) and associating the factors $(x_n - x_{n+1})$ with each denominator, the results of Table I are found.

The combined denominator designated by Q is then

$$\begin{aligned} Q &= k_1^2[x_2] + k_2^2[1 - x_4] + 2k_1 \cdot k_2[x_4 - x_2] \\ &\quad + 2k_1 \cdot [-(x_5 - x_6)(p_1 + p_2) - (x_4 - x_5)\, p_1 - (x_2 - x_3)\, p_2'] \\ &\quad + 2k_2 \cdot [(x_2 - x_3)\, p_2' - (x_1 - x_2)\, p_1'] \\ &\quad + m^2 x_6 + (x_5 - x_6)(m^2 - s) + (x_4 - x_5)(\mu^2 - m^2) + (x_3 - x_4)\, \mu^2 \\ &\quad + (x_1 - x_2)(\mu^2 - m^2) + (1 - x_1)\, m^2 \\ &= A_{11}k_1^2 + A_{22}k_2^2 + 2A_{12}k_1 \cdot k_2 + 2B_1 \cdot k_1 + 2B_2 \cdot k_2 + C. \end{aligned} \tag{19}$$

To form χ, the quantities $B_i \cdot B_j$ are required and the needed results are

$$\begin{aligned} B_1 \cdot B_1 &= -m^2[(x_4 - x_6)^2 + (x_5 - x_6)^2 + (x_2 - x_3)^2] \\ &\quad + (x_4 - x_6)(x_5 - x_6)(2m^2 - s) \\ &\quad + (x_4 - x_6)(x_2 - x_3)(u - 2m^2) + (x_5 - x_6)(x_2 - x_3)(t - 2m^2), \\ B_2 \cdot B_2 &= -m^2[(x_2 - x_3)^2 + (x_1 - x_2)^2] - (x_2 - x_3)(x_1 - x_2)(2m^2 - s), \end{aligned}$$

and

$$\begin{aligned} B_1 \cdot B_2 &= -\tfrac{1}{2}(x_4 - x_6)(x_2 - x_3)(u - 2m^2) + \tfrac{1}{2}(x_4 - x_6)(x_1 - x_2)(t - 2m^2) \\ &\quad - \tfrac{1}{2}(x_2 - x_3)(x_5 - x_6)(t - 2m^2) + \tfrac{1}{2}(x_5 - x_6)(x_1 - x_2)(u - 2m^2) \\ &\quad + m^2(x_2 - x_3)^2 + \tfrac{1}{2}(x_1 - x_2)(x_2 - x_3)(2m^2 - s). \end{aligned} \tag{20}$$

The usual invariants s, t, and u are used and they are defined by

$$\begin{aligned} s &= -(p_1 + p_2)^2, \\ t &= -(p_1 - p_1')^2, \end{aligned} \tag{21}$$

and

$$u = -(p_1 - p_2')^2.$$

Note that $s + t + u = 4m^2$.

At this point the k_i integrations may be carried out in accordance with (7) and the numerator found by (13)–(15). The result is

$$
\begin{aligned}
F = & -\frac{1}{2\pi}(g^2)^3 \int_0^1 dx_1 \int_0^{x_1} dx_2 \cdots \int_0^{x_5} dx_6 \, \Lambda \\
& \times \{\bar{u}_1 \gamma_5 [\Omega_1] \gamma_5 [\Omega_2] u_1 \, \bar{u}_2 \gamma_5 [\Omega_3] \gamma_5 [\Omega_4] \gamma_5 u_2 \qquad \chi^{-3} \\
& + \quad \gamma_\mu \quad \Omega_2 \quad \Omega_3 \quad \gamma_\mu \quad \Omega_{14} \quad \chi^{-2}/2 \\
& + \quad \gamma_\mu \quad \Omega_2 \quad \gamma_\mu \quad \Omega_4 \quad \Omega_{13} \quad \chi^{-2}/2 \\
& + \quad \gamma_\mu \quad \gamma_\mu \quad \Omega_3 \quad \Omega_4 \quad \Omega_{12} \quad \chi^{-2}/2 \\
& + \quad \Omega_1 \quad \gamma_\mu \quad \Omega_3 \quad \gamma_\mu \quad \Omega_{24} \quad \chi^{-2}/2 \\
& + \quad \Omega_1 \quad \gamma_\mu \quad \gamma_\mu \quad \Omega_4 \quad \Omega_{23} \quad \chi^{-2}/2 \\
& + \quad \Omega_1 \quad \Omega_2 \quad \gamma_\mu \quad \gamma_\mu \quad \Omega_{34} \quad \chi^{-2}/2 \\
& + \quad \gamma_\mu \quad \gamma_\mu \quad \gamma_\nu \quad \gamma_\nu \quad \Omega_{12}\,\Omega_{34}\,\chi^{-1}/2 \\
& + \quad \gamma_\mu \quad \gamma_\nu \quad \gamma_\mu \quad \gamma_\nu \quad \Omega_{13}\,\Omega_{24}\,\chi^{-1}/2 \\
& + \quad \gamma_\mu \quad \gamma_\nu \quad \gamma_\nu \quad \gamma_\mu \quad \Omega_{14}\,\Omega_{23}\,\chi^{-1}/2\}. \qquad (22)
\end{aligned}
$$

The Ω_{ij} are defined by (10), and using (11), one finds

$$\Omega_i = 2\Lambda\{\Omega_{i3} C_3 i\gamma \cdot p_2' + \Omega_{i4} C_4 i\gamma \cdot (p_1 + p_2) + \Omega_{i5} C_5 i\gamma \cdot p_1' + \Omega_{i6} C_6 i\gamma \cdot p_1\}. \qquad (23)$$

D. *Reduction to proper Amplitudes*

One remaining task is that of reducing the expressions in (22) to combinations of the five NN amplitudes. The operations required for the reduction of these expressions are quite tedious but they are straightforward. Expressions of the form

$$\bar{u}_1 \gamma_5 \Omega_1 \gamma_5 \Omega_2 \gamma_5 u_1 \,, \qquad (24)$$

can be readily reduced to

$$\bar{u}_1 \gamma_5 [A i\gamma \cdot p_2 + B] \, u_1 \,, \qquad (25)$$

by use of the properties of the γ-matrices and the Dirac equation. Combinations of the type

$$\bar{u}_1 \gamma_5 \gamma_\mu \gamma_5 \Omega_2 \gamma_5 u_1 \bar{u}_2 \gamma_5 \gamma_\mu \gamma_5 \Omega_4 \gamma_5 u_2 \qquad (26)$$

require more care. This can be written as

$$\begin{aligned} & A(\gamma_5\gamma_\mu)(\gamma_5\gamma_\mu i\gamma\cdot p_1) \\ & + B(\gamma_5\gamma_\mu i\gamma\cdot p_2)(\gamma_5\gamma_\mu) \\ & + C(\gamma_5\gamma_\mu i\gamma\cdot p_2)(\gamma_5\gamma_\mu i\gamma\cdot p_1) \\ & + D(\gamma_5\gamma_\mu)(\gamma_5\gamma_\mu) \\ & + E(\gamma_5)(\gamma_5) \\ & + F(\gamma_5 i\gamma\cdot(p_2+p_2'))(\gamma_5) \\ & + G(\gamma_5)(\gamma_5 i\gamma\cdot(p_1+p_1')). \end{aligned} \tag{27}$$

This is still not the desired form (16), so that further reduction is required. As discussed by Amati, Leader, and Vitale [15], the coefficients F and G must ultimately vanish due to TRI. Typically they are not zero at this point but vanish only after the integrations over x_i are carried out. However one can verify the TRI properties without the uncertainty of numerical integration. This is done by assigning the parameters $(x_i' - x_{i+1}')$ to the lines of the graph in such a way that on the time-reversed graph, the parameter $(x_i' - x_{i+1}')$ corresponds to the parameter $x_i - x_{i+1}$ on the analogous line of the original graph. This, of course, amounts to another choice of assignments of the parameters to the lines of the graph. An example is shown in Fig. 4.

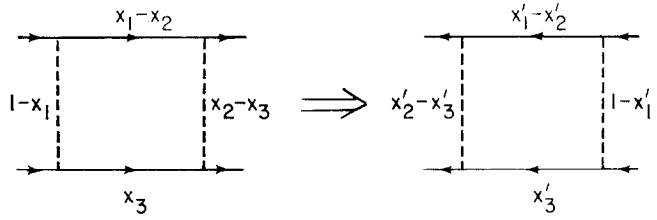

FIG. 4. Method for time-reversal-invariance check.

Using this example, one can proceed with the TRI check by evaluating the coefficients A through G with an arbitrary set of x_i, then solving for a new set of x_i' defined by

$$\begin{aligned} x_1' - x_2' &= x_1 - x_2\,, \\ x_3' &= x_3\,, \\ x_2' - x_3' &= 1 - x_1\,, \end{aligned} \tag{28}$$

and

$$1 - x_1' = x_2 - x_3\,.$$

The resulting set of values for x_i' is then used in place of the x_i to again evaluate A–G. The result is that the values of the proper amplitudes are unchanged while those which are not TRI change sign. Since the Jacobian of (28) is unity, the result is that such terms as those with coefficients F and G can be ignored after the check.

Other terms of (27) contain a γ_μ between each pair of spinors and a convenient way of reducing such terms to the form (16) is that of expanding $\gamma_\mu\gamma_\mu$ by components using a set of four orthogonal vectors in the center-of-mass system. We take these vectors to be

$$\begin{aligned} B &= p_1 - p_2 = (0, 0, 2p, 0), \\ C &= p_1 + p_2 = (0, 0, 0, 2iE), \\ A &= \cos\theta(p_1 - p_2) - (p_1' - p_2') = (-2p \sin\theta, 0, 0, 0), \end{aligned} \tag{29}$$

and

$$X_\mu = \epsilon_{\mu\nu\sigma\rho} A_\nu B_\sigma C_\rho .$$

The vector X has the property

$$i\gamma \cdot X = -i\gamma_2 A_1 B_3 C_4 = (i\gamma \cdot A)(i\gamma \cdot B)(i\gamma \cdot C)\,\gamma_5 . \tag{30}$$

The gamma matrices can now be expressed as

$$\begin{aligned} \gamma_0 &= \gamma_4 = (\gamma \cdot C)/2iE, \\ \gamma_1 &= -(\gamma \cdot A)/2p \sin\theta, \\ \gamma_2 &= (\gamma \cdot X)/8ip^2 E \sin\theta, \end{aligned} \tag{31}$$

and

$$\gamma_3 = (\gamma \cdot B)/2p.$$

One can now proceed as in this example:

$$\begin{aligned} -(\gamma_5\gamma_\mu)(\gamma_5\gamma_\mu) = &- (1/4E^2)(\gamma_5 i\gamma \cdot C)(\gamma_5 i\gamma \cdot C) \\ &+ (1/4p^2 \sin^2\theta)(\gamma_5 i\gamma \cdot A)(\gamma_5 i\gamma \cdot A) \\ &- (1/64p^4E^2 \sin^2\theta)(\gamma_5 i\gamma \cdot X)(\gamma_5 i\gamma \cdot X) \\ &+ (1/4p^2)(\gamma_5 i\gamma \cdot B)(\gamma_5 i\gamma \cdot B). \end{aligned} \tag{32}$$

Using the definitions of the vectors and the relation (30) along with the invariants in the center-of-mass system

$$\begin{aligned} s &= 4(p^2 + m^2), \\ t &= -2p^2(1 - \cos\theta), \end{aligned} \tag{33}$$

and

$$u = -2p^2(1 + \cos\theta),$$

one finds

$$\begin{aligned}(\gamma_5\gamma_\mu)(\gamma_5\gamma_\mu) = (1/stu)\{&m^2(s-u)^2\,[(1)(1)] - m^2(u^2-s^2)[(1)(i\gamma\cdot p_1) + (i\gamma\cdot p_2)(1)]\\ &+ (s+u)^2\,[(i\gamma\cdot p_2)(i\gamma\cdot p_1)]\\ &+ t(u-s)\left[\left(\gamma_5 i\gamma\cdot\left(\frac{p_2+p_2'}{2}\right)\right)\left(\gamma_5 i\gamma\cdot\left(\frac{p_1+p_1'}{2}\right)\right)\right]\\ &- 4m^2 su\,[(\gamma_5)(\gamma_5)]\}.\end{aligned} \tag{34}$$

A complete set of such relations is given in the appendix.

Expressions from (22) which contain a pair of γ_μ factors between the same spinors are readily reduced by the properties of the γ-matrices. However the last two terms in (22) are different. These terms such as

$$(\gamma_5\gamma_\mu\gamma_5\gamma_\nu\gamma_5)(\gamma_5\gamma_\mu\gamma_5\gamma_\nu\gamma_5), \tag{35}$$

can be reduced by noting that

$$\gamma_5\gamma_\mu\gamma_5\gamma_\nu\gamma_5 = \begin{cases}\gamma_5 & \text{if } \nu = \mu\\ \gamma_\alpha\gamma_\beta & \text{if } \nu \neq \mu \text{ where } \alpha \neq \beta \text{ and } \alpha, \beta \neq \mu, \nu.\end{cases} \tag{36}$$

Thus one finds

$$(\gamma_5\gamma_\mu\gamma_5\gamma_\nu\gamma_5)(\gamma_5\gamma_\mu\gamma_5\gamma_\nu\gamma_5) = 4(\gamma_5)(\gamma_5) - 2\sum_{\mu>\nu}(i\gamma_\mu\gamma_\nu)(i\gamma_\mu\gamma_\nu). \tag{37}$$

The second term is the tensor combination which can be written in the form (16) using the results of Amati *et al.* [15] as given in the appendix.

E. *Integration*

At the conclusion of the manipulations in the last section, one has expressions for the five amplitudes of the form

$$A_j = \int_0^1 dx_1 \cdots \int_0^{x_5} dx_6\, \Delta f_j(x_i, s, t)[\chi(x_i, s, t)]^{-3}. \tag{38}$$

The only practical means of evaluating such multiple integrals is by Monte Carlo methods. Unfortunately the integrands generally are not very smooth functions so it is desirable to optimize the procedure beyond simple random sampling over the region of integration.

In order to improve on the Monte Carlo method, we have first made the following change of variable:

$$\begin{aligned} x_1 &= y_1^{1/n}, \\ x_2 &= x_1(1 - y_2)^{1/(n-1)}, \\ x_3 &= x_2(1 - y_3)^{1/(n-2)}, \\ &\vdots \\ x_n &= x_{n-1}(1 - y_n), \end{aligned}$$

so that each of the new variables runs over the range zero-to-one and we have divided the resulting hypercubic integration region into a set of hypercubes of equal volume. We then deal with each hypercube individually. Thus if there are n integration variables and each dimension is divided into m units, there will be m^n such cubes. The Monte Carlo method is then applied to each cube so that the total estimated error is minimized subject to the condition that the total number of trials is fixed at N.

If σ_i denotes the estimated standard deviation in the i-th cube in which N_i samples are taken, then

$$\sigma_i^2 = \left(\sum_{n=1}^{N_i} f_n^2 - \left(\sum_{n=1}^{N_i} f_n\right)^2 / N_i\right) / N_i = \overline{f^2} - (\bar{f})^2. \tag{39}$$

For a well-behaved integrand, the rate of convergence of the Monte Carlo method is proportional to $N_i^{1/2}$. The error estimate is

$$(\text{Error})^2 = \sum_{i=1}^{m^n} \sigma_i^2 / N_i \,. \tag{40}$$

Thus in order to minimize the error subject to the condition that $N = \sum N_i$ is fixed, it must be the case that

$$N_i \propto \sigma_i \,. \tag{41}$$

Accordingly we have adopted the following procedure:

(a) Divide the region into m^n hypercubes.

(b) Estimate σ_i by using an equal number of samples in each hypercube.

(c) Integrate each hypercube independently by the Monte Carlo method using $N_i \propto \sigma_i$ and add the results appropriately.

This procedure may be iterated as many times as needed to obtain the desired precision. Generally it is found that this method is superior to the straightforward

Monte Carlo method because relatively few of the hypercubes give a major contribution to the error.

Another problem is that presented by the unitary cuts arising at the elastic threshold for the graphs of Figs. 1(e) and 1(f). As a function of s, the amplitudes for these graphs have cuts for $s > 4m^2$ and this makes the evaluation of the amplitudes difficult due to the singularity of the integrand. In order to handle this problem we evaluate the amplitudes off the axis by changing s to $s + i\epsilon$ and then attempting to extrapolate to $\epsilon = 0$.

The quantity χ appearing in the integrand is linear in s and it can vanish, thus producing the singularity and the cut. Writing χ as

$$\chi = h(x_i) + sg(x_i), \tag{42}$$

and introducing $s \to s + i\epsilon$, the real part of the amplitude A_j of (38) becomes

$$\text{Re } A_j = \lim_{\epsilon \to 0} \int dx_i \, Af_j \frac{\chi^3 - 3\chi g^2 \epsilon^2}{[\chi^3 - 3\chi g^2 \epsilon^2]^2 + [3\chi^2 g\epsilon - \epsilon^3 g^3]^2}. \tag{43}$$

The integral is now well defined for $\epsilon > 0$ and the only question remaining is that of investigating numerically the behavior as a function of ϵ to determine whether or not the extrapolation to $\epsilon = 0$ is feasible.

These methods may satisfactorily provide the full amplitudes but in order to properly evaluate the results, the contributions to the partial-wave amplitudes are required. Therefore one needs a partial-wave projection which will require an additional integration over angle. Furthermore, the five amplitudes must be combined appropriately to describe transitions among the usual states.

The A_j coefficients can be related to the F_j coefficients of Goldberger, Grisaru, McDowell, and Wong [16] where the F_j coefficients are defined by

$$F = F_1(S - \tilde{S}) + F_2(T + \tilde{T}) + F_3(A - \tilde{A}) + F_4(V + \tilde{V}) + F_5(P - \tilde{P}). \tag{44}$$

Details are given in the Appendix.

In terms of the F_i coefficients, the partial-wave projection of the singlet amplitude is

$$h_J = \frac{1}{2} \int_{-1}^{1} d(\cos\theta) \, P_J(\cos\theta) \frac{1}{8\pi} \{(E^2 + m^2) F_1 - 2p^2 F_2 \cos\theta - (3E^2 + 3m^2 + p^2) F_3 + p^2 F_5\}. \tag{45}$$

h_J is related to the singlet phase shift by

$$h_J = (E/2\text{imp})(e^{2i\delta_J} - 1). \tag{46}$$

The results for the other amplitudes are given in the Appendix.

In order to compute h_J it is efficient to combine the integrands for the F_i amplitudes according to (45) and then integrate them all at once. It should be expected that the accuracy with which a given partial-wave amplitude can be found will decrease with increasing J since the magnitude of the partial-wave amplitudes decreases with increasing J while the error remains fixed.

Two methods have been used to carry out the partial-wave projections. For cases in which the estimated error of the full amplitudes was less than about 1 %, the integrals over angle were carried out by Gaussian quadrature. In cases of limited accuracy a useful procedure was found to be that of taking appropriate sums of the full amplitude evaluated at definite values of $\cos\theta$. For example, if one needs the $l = 1$ part of

$$f(z) = f_0 + 3f_1P_1(z) + 5f_2P_2(z) + 7f_3P_3(z) + \cdots, \tag{47}$$

then

$$f_1 \cong [f(z_3) - f(-z_3)]/6P_1(z_3), \tag{48}$$

where $P_3(\pm z_3) = 0$.

F. *Other Graphs*

The methods discussed are readily applicable to those graphs of Fig. 1(e)–(h). The graphs of Fig. 1(i) and (j) are somewhat different and they present other problems as regards the spinor algebra. Using the procedure indicated earlier, the "basic term" for these graphs is

$$\bar{u}_1\gamma_5\Omega_1\gamma_5\Omega_2\gamma_5\Omega_3\gamma_5u_1\bar{u}_2\gamma_5\Omega_4\gamma_5u_2\,. \tag{49}$$

Following the substitution procedure, the integrand will be of the form

$$\begin{array}{lccccc}
 & \bar{u}_1\gamma_5[\Omega_1] & \gamma_5[\Omega_2] & \gamma_5[\Omega_3] & \gamma_5u_1\bar{u}_2\gamma_5[\Omega_4] & \gamma_5u_2 \quad \chi^{-3} \\
+ & \gamma_\mu & \gamma_\mu & \Omega_3 & \Omega_4 & \Omega_{12}\chi^{-2}/2 \\
+ & \gamma_\mu & \Omega_2 & \gamma_\mu & \Omega_4 & \Omega_{13}\chi^{-2}/2 \\
+ & \gamma_\mu & \Omega_2 & \Omega_3 & \gamma_\mu & \Omega_{14}\chi^{-2}/2 \\
+ & \Omega_1 & \gamma_\mu & \gamma_\mu & \Omega_4 & \Omega_{23}\chi^{-2}/2 \\
+ & \Omega_1 & \gamma_\mu & \Omega_3 & \gamma_\mu & \Omega_{24}\chi^{-2}/2 \\
+ & \Omega_1 & \Omega_2 & \gamma_\mu & \gamma_\mu & \Omega_{34}\chi^{-2}/2 \\
+ & \gamma_\mu & \gamma_\mu & \gamma_\nu & \gamma_\nu & \Omega_{12}\Omega_{34}\chi^{-1}/2 \\
+ & \gamma_\mu & \gamma_\nu & \gamma_\mu & \gamma_\nu & \Omega_{13}\Omega_{24}\chi^{-1}/2 \\
+ & \gamma_\mu & \gamma_\nu & \gamma_\nu & \gamma_\mu & \Omega_{14}\Omega_{23}\chi^{-1}/2.
\end{array} \tag{50}$$

Since an even number of γ_5's occur between pairs of spinors, all γ_5's can be

eliminated in favor of some changes of sign. Consequently, terms of the form

$$\bar{u}_1\gamma_5[\text{factor containing 0 or } 2\gamma_\mu\text{'s}]\,\gamma_5 u_1\bar{u}_2\gamma_5\Omega_4\gamma_5 u_2 \tag{51}$$

can readily be reduced to

$$\bar{u}_1[Ai\gamma\cdot p_2 + B]\,u_1\bar{u}_2[Ci\gamma\cdot p_1 + B]\,u_2\,. \tag{52}$$

Terms of the form

$$\bar{u}_1\gamma_5[\text{factor containing } 1\gamma_\mu]\,\gamma_5 u_1\bar{u}_2\gamma_5\gamma_\mu\gamma_5 u_2\,, \tag{53}$$

can be written as

$$\begin{aligned} &A\bar{u}_1\gamma_\mu u_1\bar{u}_2\gamma_\mu u_2\\ &+ B\bar{u}_1 i\gamma\cdot p_2 u_1\bar{u}_2 i\gamma\cdot p_1 u_2\\ &+ C\bar{u}_1 i\gamma\cdot p_2 u_1\bar{u}_2 u_2\\ &+ D\bar{u}_1 u_1 u_2 i\gamma\cdot p_1 u_2\\ &+ E\bar{u}_1 u_1\bar{u}_2 u_2\\ &+ F\bar{u}_1\gamma_\mu i\gamma\cdot p_2 u_1\bar{u}_2\gamma_\mu u_2\,. \end{aligned} \tag{54}$$

All terms except that with coefficient F are in the standard form (16) and it can be handled as indicated in the appendix.

Finally the last three terms of (50) can be reduced to

$$\bar{u}_1\gamma_\mu u_1\bar{u}_2\gamma_\mu u_2\,, \tag{55}$$

and the reduction is complete.

The graphs of Fig. 1(a)–(d) are of a different character from those already discussed in that they result from the $\lambda\phi^4$ interaction. The graph of Fig. 1(a) is easily handled using the technique of Anderson, Gupta, and Huschilt [17]. The result is

$$F = -\frac{1}{2}\lambda(g^2)^2\frac{m^2}{\pi^2\mu^4}\left[\int_0^1 dx\,\frac{\mu^2(1-x)}{kz}\ln\left(\frac{2z+kx}{2z-kx}\right)\right]^2\bar{u}_1u_1\bar{u}_2u_2\,, \tag{56}$$

where $k = \sqrt{-t}$ and $z = [u^2x + m^2(1-x)^2 + k^2x^2/4]^{1/2}$. Since only one integration is required, this amplitude is easily computed with sufficient precision to allow projection of the required partial waves.

The other graphs containing the $\lambda\phi^4$ interaction are more difficult, partly because they must be renormalized. Consider the graphs of Fig. 5. The graph of Fig. 5(a) requires a renormalization due to the internal loop. The procedure for such a renormalization requires that the loop shown in Fig. 6 be subtracted

so that it gives no contribution at the symmetry point $s = t = u = 4/3\mu^2$. Here s, t, and u are taken as if the loop in Fig. 6 were external, that is $s = -(k_1 + k_3)^2$. Consequently, the amplitude for Fig. 5(a) is renormalized by subtracting the amplitude for Fig. 5(b) evaluated at $Q^2 = -4/3\mu^2$, treating Q as an external momentum. The graph of Fig. 5(c) must also be evaluated and comparing it with

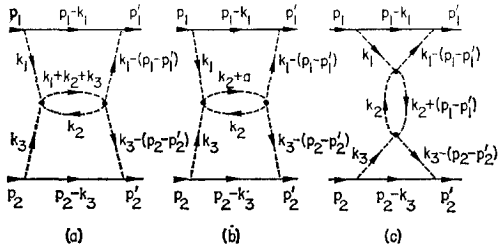

FIG. 5. Graphs used for the λ renormalization.

Fig. 5(b), it is clear that (c) is given from (b) using $Q = p_1 - p_1'$. The remaining graph of Fig. 1(d) is related by crossing symmetry to that of Fig. 5(a). That is, upon the interchange $p_2 \rightleftarrows -p_2'$ or, equivalently, $s \rightleftarrows u$ plus changes of sign of the coefficients A_2 and A_4 in (16), the amplitude for Fig. 5(a) is changed to that for Fig. 1(d).

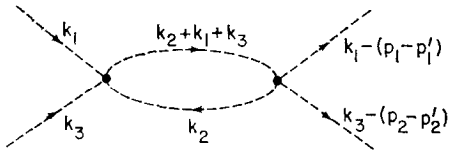

FIG. 6. Internal loop.

The amplitude for the graph of Fig. 5(a) is

$$F^a = 2ig^4\lambda^2/\pi^8 \int d^4k_1 d^4k_2 d^4k_3 \frac{\bar{u}_1\gamma_5[i\gamma\cdot(p_1 - k_1) - m]\,\gamma_5 u_1}{[(p_1 - k_1)^2 + m^2][k_1^2 + \mu^2]}$$
$$\times \frac{\bar{u}_2\gamma_5[i\gamma\cdot(p_2 - k_3) - m]\,\gamma_5 u_2}{[(k_1 - (p_1 - p_1')^2 + \mu^2][(k_1 + k_2 + k_3)^2 + \mu^2][k_2^2 + \mu^2]}$$
$$\times \frac{1}{[(p_2 - k_3)^2 + m^2][k_3^2 + \mu^2][(k_3 - (p_2 - p_2'))^2 + \mu^2]}. \tag{57}$$

Assigning the Feynman parameters in the order of appearance of the propagators in (57) so that the first has a coefficient x_7, the second $(x_6 - x_7)$, etc., and assigning the momenta P^i, the results of Table II are found.

TABLE II

Parameters associated with the graphs considered for the renormalization

i	1	2	3	4	5*
C_i	x_7	$x_2 - x_3$	$x_5 - x_6$	$1 - x_1$	$x_4 - x_5$
∂_{i1}	-1	0	-1	0	0
∂_{i2}	0	0	0	0	1
∂_{i3}	0	-1	0	-1	0
P^i	p_1	p_2	$p_1 - p_1'$	$p_2 - p_2'$	Q

The parameters occurring in the expression (9) for χ are

$$\begin{aligned} A_{11} &= x_4, & A_{13} &= x_4 - x_5, \\ A_{22} &= x_3 - x_5, & A_{23} &= x_4 - x_5, \\ A_{33} &= x_4 - x_5 + 1 - x_3, & A_{12} &= x_4 - x_5, \end{aligned}$$

$$\begin{aligned} B_1 &= -x_7 p_1 - (x_5 - x_6)(p_1 - p_1'), \\ B_2 &= 0, \\ B_3 &= -(x_2 - x_3)\, p_2 - (1 - x_1)(p_2 - p_2'), \end{aligned} \tag{58}$$

and

$$C = \mu^2(x_3 - x_7 + 1 - x_2) - t(x_5 - x_6 + 1 - x_1).$$

Following Chisholm's method, we find

$$\begin{aligned} F^a = 2g^4\lambda^2/\pi \int dx_i \{ & \bar{u}_1\gamma_5\Omega_1\gamma_5 u_1 \bar{u}_2\gamma_5\Omega_2\gamma_5 u_2 \chi^{-2} \\ & + \bar{u}_1\gamma_5\gamma_\mu\gamma_5 u_1 \bar{u}_2\gamma_5\gamma_\mu\gamma_5 u_2 \Omega_{12}\chi^{-1}\}. \end{aligned} \tag{59}$$

Noting the form of Ω_i from (11), it is apparent that by use of the Dirac equation we can write

$$\begin{aligned} F^a = {} & A[\bar{u}_1 u_1 \bar{u}_2 u_2] + B[\bar{u}_1 i\gamma \cdot p_2 u_1 \bar{u}_2 i\gamma \cdot p_1 u_2] \\ & + C[\bar{u}_1 i\gamma \cdot p_2 u_1 \bar{u}_2 u_2] + D[\bar{u}_1 u_1 \bar{u}_2 i\gamma \cdot p_2 u_2] \\ & + E[\bar{u}_1\gamma_\mu u_1 \bar{u}_2\gamma_\mu u_2]. \end{aligned} \tag{60}$$

Considering the graph of Fig. 5(c), which is equivalent to that of Fig. 5(b), it is seen that its amplitude will contribute only a coefficient to the "scalar" spinor

combination $\bar{u}_1 u_1 \bar{u}_2 u_2$. Consequently, only one of the terms of (60) requires renormalization. This renormalization is conveniently done by evaluating the amplitude of Fig. 5(b) in a manner parallel to that used for Fig. 5(a). The only difference is that the momentum Q is treated as an external momentum so that there are five P^i's rather than four. The associated parameters are also given in Table II. The parameters needed for forming χ are the same as in (58) except that now

$$A_{11} = x_5, \qquad A_{ij} = 0 \quad (i \neq j),$$
$$A_{33} = 1 - x_3, \qquad B_2 = (x_4 - x_5)Q, \tag{61}$$

and

$$C = \mu^2(x_3 - x_7 + 1 - x_2) - t(x_5 - x_6 + 1 - x_1) + Q^2(x_4 - x_5).$$

Equation (59) holds equally well for F^b except for the changes in χ, Ω_i, and Ω_{ij}. Evaluating the required expression it is found that $\Omega^b_{12} = 0$ and that Q does not appear in the numerator. In fact, this contributes only to the scalar amplitude and F^b can be written as

$$F^b = 2m^2 g^4 \lambda^2/\pi^2 \, \bar{u}_1 u_1 \bar{u}_2 u_2 \int dx_i \frac{x_7(x_2 - x_3)}{x_5(1 - x_3)\chi^2}. \tag{62}$$

The renormalized amplitude for the graph of Fig. 5(a) is

$$F_R{}^a = F^a - F^b(Q^2 = -4/3\mu^2), \tag{63}$$

and that for Fig. 5(c) is

$$F_R{}^c = F^b(Q^2 = -t) - F^b(Q^2 = -4/3\mu^2). \tag{64}$$

Finally the amplitude for the remaining graph of Fig. 1(d) is

$$F = F_R{}^a(\text{with } s \rightleftarrows u \text{ plus a sign change of } A_2 \text{ and } A_4). \tag{65}$$

Since F^a and F^b are evaluated using the same assignments of Feynman parameters, the required renormalizations can be done by simply subtracting the integrands.

The integrands for these graphs contain not only the singularity requiring renormalization but also boundary singularities which occur when some combinations of the Feynman approach their extreme values. These singularities are integrable but some are too severe to be handled by Monte Carlo methods. In order to control this situation, we have made a change of variable suited to handle integrals of the type

$$\int_0^1 \frac{dx}{\sqrt{x(1-x)}}. \tag{66}$$

This integral has integrable singularities at the end points and it is unsuitable for Monte Carlo integration. To correct this we seek a new variable y such that

$$\begin{aligned} &y(x = 0) = 0, \qquad (\partial x/\partial y)(x = 0) = 0, \\ \text{and} \qquad &y(x = 1) = 1, \qquad (\partial x/\partial y)(x = 1) = 0. \end{aligned} \tag{67}$$

The derivative conditions are satisfied if

$$\partial x/\partial y \sim y(1 - y), \qquad \text{or} \qquad x \sim y^2/2 - y^3/3. \tag{68}$$

The other conditions then imply

$$x = 3y^2 - 2y^3. \tag{69}$$

Now as $y \to 0$, $x(y) \to 3y^2$ and the integrand approaches a constant. Similarly for $y \to 1$. In the same manner one could use

$$\partial x/\partial y = y^2(1 - y)^2, \tag{70}$$

giving

$$x = 10y^3 - 15y^4 + 6y^5.$$

This method is applied by making the same transformation on all the Feynman parameters independently and it results in a smoothing of the integrand in spite of the fact that the singularities are not exactly of the form (66).

G. *Branch Cut Singularity*

The amplitude for the graph of Fig. 3 has a branch cut as a function of the energy variable s beginning at the elastic threshold. Earlier we described the $s \to s + i\epsilon$ method of handling this difficulty. However, it is found that a more powerful technique is required to obtain results of reasonable accuracy. The branch cut appears in the Feynman parametric integral as a pole in the integrand and after the substitution $s \to s + i\epsilon$ there remains a large ridge in the integrand making numerical integration difficult.

The denominator is of the form χ^3 so that there is a singularity at $\chi = 0$. Now χ is quadratic in x_1, so that we can write

$$\chi = ax_1^2 + bx_1 + c, \tag{71}$$

where a, b, and c are functions of the remaining x_i as well as s and t.

Since χ is to the third power, the sign of the integrand is different on opposite sides of the singular hypersurface $\chi = 0$. We want to exploit this fact by employing a procedure which, upon encountering a point near the singular surface, averages with the resulting value, the value of opposite sign taken from the "other side" of the surface. Great care must be taken to assure that the method of finding the opposite point is symmetric. That is, there must be a one-to-one correspondence between the points. Our procedure is as follows:

(a) Choose a random number vector $(x_1, x_2, ..., x_7)$.

(b) Taking x_2 through x_7 as fixed, solve $\chi = 0$ giving either 2 or 0 real roots.

(c) If the roots are complex, proceed in the usual way.

(d) If the roots are real, find the one closer to x_1 and call it Root 1.

(e) Find the point on the opposite side of the $\chi = 0$ surface by $x_1^f = x_1 + 2(\text{Root } 1 - x_1)$.

(f) Check to see if x_1^f is in the region $1 > x_1^f > x_1$. If not, disregard x_1^f and proceed in the usual way.

(g) Check to see if x_1^f is closer to Root 1 than to the other root. If not, disregard x_1^f and proceed in the usual way.

(h) Evaluate the integrand at the two points $(x_1, x_2, ..., x_7)$ and $(x_1^f, x_2, ..., x_7)$ and average the results.

This procedure has been used in conjunction with the transformation of (69) for boundary singularities. This requires that the contribution from $(x_1^f, x_2, ..., x_7)$ be weighted according to the changed Jacobian since the Jacobian depends on x_1. In order to do this, it is necessary to solve the cubic equation (69) for y.

H. *Isospin*

Up to this point nothing has been said concerning the isospin structure of the amplitudes. Each graph gives a possibly different contribution to the isospin 0 and 1 states of the two nucleons. The interaction Hamiltonian with full isospin structure is

$$I = \delta_{ij} i(4\pi)^{1/2} g\bar{N}\gamma_5\tau_i N\phi_j + 4\pi\lambda(\delta_{ij}\delta_{kl} + \delta_{ik}\delta_{jl} + \delta_{il}\delta_{jk})\,\phi_i\phi_j\phi_k\phi_l\,. \quad (72)$$

The isospin wavefunctions in terms of the individual particle states is shown in Table III. Using this information one finds that the isospin factor, for example, for the graph of Fig. 1(e) in the $I = 1$, $I_3 = 1$ state is

$$\sum_{ijk} \chi_+^\dagger(1)[\tau_i\tau_j\tau_k]\,\chi_+(1)\,\chi_+^\dagger(2)[\tau_i\tau_j\tau_k]\,\chi_+(2). \quad (73)$$

For the $I = 0$, $I_3 = 0$ state the result is

$$\begin{aligned}\tfrac{1}{2}\sum_{ijk}\,&[\chi_+^\dagger(1)[\tau_i\tau_j\tau_k]\,\chi_+(1)\,\chi_-^\dagger(2)[\tau_i\tau_j\tau_k]\,\chi_-(2)\\&+\chi_-^\dagger(1)[\tau_i\tau_j\tau_k]\,\chi_-(1)\,\chi_+^\dagger(2)[\tau_i\tau_j\tau_k]\,\chi_+(2)\\&-\chi_+^\dagger(1)[\tau_i\tau_j\tau_k]\,\chi_-(1)\,\chi_-^\dagger(2)[\tau_i\tau_j\tau_k]\,\chi_+(2)\\&-\chi_-^\dagger(1)[\tau_i\tau_j\tau_k]\,\chi_+(1)\,\chi_+^\dagger(2)[\tau_i\tau_j\tau_k]\,\chi_-(2)].\end{aligned}\tag{74}$$

The factors for the graphs of Fig. 1(f)–(h) are similar except for the ordering of the indices on the second set of τ's.

TABLE III

Isospin states where 1 or 2 labels the two particles and where $\chi_+ = \binom{1}{0}$ and $\chi_- = \binom{0}{1}$

I	I_3	χ_{total}
1	1	$\chi_+(1)\chi_+(2)$
1	0	$1/\sqrt{2}(\chi_+(1)\chi_-(2) + \chi_-(1)\chi_+(2))$
1	−1	$\chi_-(1)\chi_-(2)$
0	0	$1/\sqrt{2}(\chi_+(1)\chi_-(2) - \chi_-(1)\chi_+(2))$

TABLE IV

Isospin factors associated with the graphs

Figure	$I = 1$	$I = 0$
1(a)	15	15
1(b)	75	75
1(c)	75	75
1(d)	75	75
1(e)	1	−27
1(f)	5	9
1(g)	−7	−3
1(h)	13	−15
1(i)	11	3
1(j)	7	15

For the graphs of Fig. 1(i) and (j), the combinations of τ's occurring in the brackets become

$$[\tau_i\tau_j\tau_k\tau_i]_1\,[\tau_j\tau_k]_2 \quad \text{and} \quad [\tau_i\tau_j\tau_k\tau_i]_1\,[\tau_k\tau_j]_2\,, \quad \text{respectively.} \tag{75}$$

The graph of Fig. 1(a) gives an isospin factor of

$$[\tau_i\tau_j]_1\,[\tau_k\tau_l]_2\,(\delta_{ij}\delta_{kl} + \delta_{ik}\delta_{jl} + \delta_{il}\delta_{jk}), \tag{76}$$

while the remaining graphs of Fig. (b)–(d) give

$$[\tau_i\tau_j]_1\,[\tau_k\tau_l]_2\,(\delta_{ij}\delta_{mn} + \delta_{im}\delta_{jn} + \delta_{in}\delta_{mj}) \times (\delta_{kl}\delta_{mn} + \delta_{km}\delta_{ln} + \delta_{kn}\delta_{ml}). \tag{77}$$

Evaluating all these expressions, the results of Table IV are found.

III. Results

Evaluation of the sixth-order ladder graph of Fig. 1(e) by the techniques described requires an extrapolation to $\epsilon = 0$. An example of this extrapolation is shown in Fig. 7. One sees that this extrapolation is very uncertain and it is

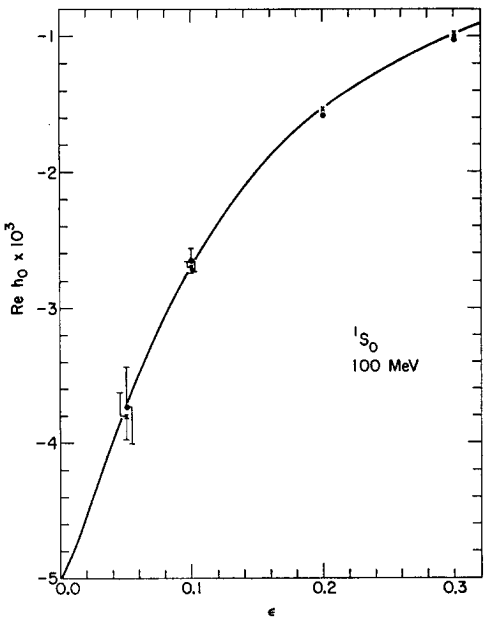

Fig. 7. Example of the extrapolation for the case of the sixth-order ladder graph in the $^1S_0$ state. The · and × represent results of the first and second iterations.

suited only for order of magnitude estimates. Consequently we have used the results of a calculation in which the Bethe-Salpeter equation is iterated [18] to find the ladder graph amplitudes. We can give only the $^1S_0$ and $^3P_0$ amplitudes. The $\epsilon = 0$ point of Fig. 7 is provided by the Bethe–Salpeter calculation.

For the graph of Fig. 1(f) the extrapolation is much better as demonstrated by Fig. 8. Still a precision of no more than 10 % can be achieved so that the extraction of partial-wave amplitudes will be limited.

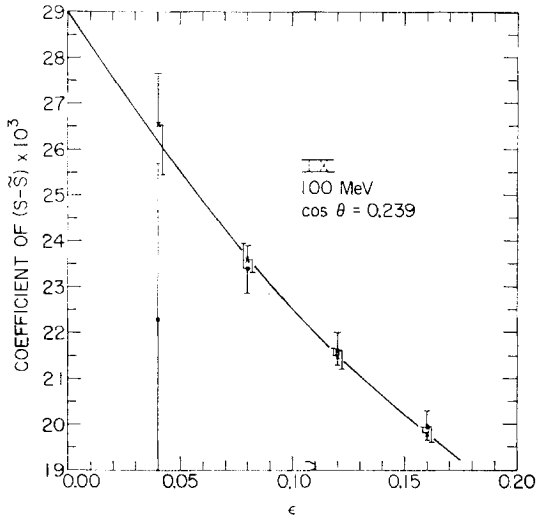

FIG. 8. Example of the extrapolation of the dominant part of the full amplitude of a singular sixth-order graph. The · and × represent results of the first and second iteration.

It is important to note that any reducible graph (graph with a two particle cut), including 1(f), can be calculated by putting the irreducible parts into a Bethe–Salpeter kernel [20].

The graphs of Fig. 1(b)–(d) have integrable singularities at some boundaries and a prescription for improving this situation was described in the last section. The results of this modification are such that for the graph of Fig. 1(b) a great improvement is realized. This is shown in Table V.

We have found that in order to produce usable partial-wave amplitudes through G waves, it is necessary that the error in the full amplitude will be less than 1 %. This is am empirical conclusion based on the observation of the stability of the partial-wave amplitudes while increasing the number of Monte Carlo points.

The procedure of dividing the region into hypercubes and assigning the number of Monte Carlo points according to the relative error is found to be valuable. Typically, for the suitable cases, it is found that the error estimate for the ampli-

TABLE V

Effects of the transformation used for integrable boundary singularities

Transformation	Error estimate
$x = y$	24%
$x = 3y^2 - 2y^3$	3.6%
$x = 10y^3 - 15y^4 + 6y^5$	3.0%

tudes improves by better than a factor of two upon going to the second iteration. This contrasts with the expected improvement of a factor of $\sqrt{2}$ for the usual Monte Carlo doubling of the number of points. However, this procedure takes up time that could be used for the usual method so that it must be fairly effective to merit its use. For smoother integrands such a procedure is not efficient since its effect is that of nearly maintaining the already smooth distribution.

In order to extract the real part of the amplitude for the graph of Fig. 3, we have used $s \to s + i\epsilon$ and sampled on either side of the singular surface. This method of dealing with the singular surface has given a great improvement over the $s \to s + i\epsilon$ method, especially when used in conjunction with the method of hypercubes discussed in the last paragraph. It would not have been practical to attempt to evaluate such an integral without some such method for dealing with the integrand with such large peaks. Still we have only been able to extract useful information for the $J = 0$, 1, and 2 cases.

The numerical results of this calculation are given in Tables VI–VIII. The units are such that $m = \hbar = c = 1$. $E = \sqrt{p^2 + m^2}$ and $(p/m)^2 = E_{LAB}/2m$. It is important to note that a factor 2 due to the Pauli principle is not included in the tabulated numbers. As an example of conversion to move standard quantities, we convert the results of Ref. [18] to the results tabulated in Table VII ($E_{LAB} = 100$ MeV) for the $^1S_0$ case. In this paper, Table VII gives for OPE + Box graph,

$$\mathrm{Re}\, h_0(^1S_0) = -0.0947\, g^2 + 0.0250\, g^4 + \cdots,$$

which does not include a factor 2 due to the Pauli principle. In reference 18, in Table VIII for the 15 × 15 mesh, $^1S_0$ state,

$$\tan \delta(^1S_0) = -0.04263\, g^2 + 0.0126\, g^4 + \cdots.$$

In reference 18, we used a g^2 such that $g^2/4\pi = 14$, and in the present we use a g^2

TABLE

Values of the real parts of

	OPE	BOX	X-BOX	1(a)	1(b)	1(c)
$^1S_0$	$-.798\times10^{-1}$	$.251\times10^{-1}$	$.374\times10^{-1}$	$-.469\times10^{0}$	$-.41\times10^{0}$	$-.17\times10^{1}$
$^3P_0$	$.798\times10^{-1}$	$.371\times10^{-2}$	$-.238\times10^{-2}$	$-.190\times10^{-1}$	$.54\times10^{-1}$	$-.36\times10^{-1}$
$^1P_1$	$-.382\times10^{-1}$	$.236\times10^{-2}$	$-.117\times10^{-2}$	$-.231\times10^{-1}$	$.50\times10^{0}$	$-.67\times10^{-1}$
$^3P_1$	$-.463\times10^{-1}$	$.124\times10^{-2}$	$.757\times10^{-3}$	$-.210\times10^{-1}$	$.52\times10^{-1}$	$-.54\times10^{-1}$
$^3S_1$	$-.798\times10^{-1}$	$.202\times10^{-0}$	$-.247\times10^{-1}$	$-.469\times10^{0}$	$-.41\times10^{0}$	$-.17\times10^{1}$
$^3D_1$	$-.208\times10^{-1}$	$-.799\times10^{-3}$	$-.362\times10^{-4}$	$-.190\times10^{-2}$	$.64\times10^{-2}$	$-.45\times10^{-2}$
ϵ_1	$.835\times10^{-1}$	$-.379\times10^{-2}$	$-.398\times10^{-3}$	$.635\times10^{-5}$	$.6\times10^{-5}$	$-.21\times10^{-2}$
$^1D_2$	$.428\times10^{-2}$	$.269\times10^{-4}$	$.142\times10^{-3}$	$-.208\times10^{-2}$	$.68\times10^{-2}$	$-.54\times10^{-2}$
$^3D_2$	$.294\times10^{-1}$	$.535\times10^{-3}$	$-.660\times10^{-4}$	$-.202\times10^{-2}$	$.67\times10^{-2}$	$-.51\times10^{-2}$
$^3P_2$	$.416\times10^{-2}$	$.594\times10^{-3}$	$.140\times10^{-2}$	$-.251\times10^{-1}$	$.48\times10^{-1}$	$-.73\times10^{-1}$
$^3F_2$	$.135\times10^{-2}$	$-.272\times10^{-5}$	$.901\times10^{-5}$	$-.216\times10^{-3}$	$.9\times10^{-3}$	$-.5\times10^{-3}$
ϵ_2	$-.689\times10^{-2}$	$-.144\times10^{-4}$	$.154\times10^{-4}$	$.211\times10^{-6}$	$-.4\times10^{-6}$	$-.7\times10^{-4}$
$^1F_3$	$-.461\times10^{-2}$	$.273\times10^{-4}$	$-.864\times10^{-5}$	$-.232\times10^{-3}$	$.9\times10^{-3}$	$-.6\times10^{-3}$
$^3F_3$	$-.284\times10^{-2}$	$.541\times10^{-5}$	$.123\times10^{-4}$	$-.228\times10^{-3}$	$.9\times10^{-3}$	$-.5\times10^{-3}$
$^3D_3$	$-.289\times10^{-2}$	$.383\times10^{-3}$	$-.767\times10^{-4}$	$-.221\times10^{-2}$	$.7\times10^{-3}$	$-.6\times10^{-2}$
$^3G_3$	$-.102\times10^{-2}$	$-.307\times10^{-7}$	$-.709\times10^{-6}$	$-.278\times10^{-4}$	$.1\times10^{-3}$	$-.6\times10^{-4}$
ϵ_3	$.650\times10^{-2}$	$-.100\times10^{-4}$	$-.662\times10^{-6}$	$.134\times10^{-7}$	$-.4\times10^{-7}$	$-.4\times10^{-5}$
$^1G_4$	$.571\times10^{-3}$	$.388\times10^{-6}$	$.170\times10^{-5}$	$-.295\times10^{-4}$	$.1\times10^{-3}$	$-.7\times10^{-4}$
$^3G_4$	$.280\times10^{-2}$	$.567\times10^{-5}$	$-.897\times10^{-6}$	$-.291\times10^{-4}$	$.1\times10^{-3}$	$-.7\times10^{-4}$
$^3F_4$	$.264\times10^{-3}$	$.428\times10^{-5}$	$.133\times10^{-4}$	$-.244\times10^{-3}$	$.9\times10^{-3}$	$-.6\times10^{-3}$
$^3H_4$	$.969\times10^{-4}$	$.266\times10^{-7}$	$.161\times10^{-6}$	$-.390\times10^{-5}$	$.2\times10^{-4}$	$-.8\times10^{-5}$
ϵ_4	$-.747\times10^{-3}$	$-.116\times10^{-6}$	$.108\times10^{-6}$	$.115\times10^{-8}$	$-.4\times10^{-8}$	$-.4\times10^{-6}$
$^1H_5$	$-.652\times10^{-3}$	$.486\times10^{-6}$	$-.132\times10^{-6}$	$-.410\times10^{-5}$	$.2\times10^{-4}$	$-.9\times10^{-5}$
$^3H_5$	$-.326\times10^{-3}$	$.829\times10^{-7}$	$.197\times10^{-6}$	$-.406\times10^{-5}$	$.2\times10^{-4}$	$-.9\times10^{-5}$
$^3G_5$	$-.238\times10^{-3}$	$.459\times10^{-5}$	$-.954\times10^{-6}$	$-.309\times10^{-4}$	$.1\times10^{-3}$	$-.7\times10^{-4}$
$^3I_5$	$-.896\times10^{-4}$	$.595\times10^{-7}$	$-.137\times10^{-7}$	$-.120\times10^{-5}$	$.3\times10^{-5}$	$-.1\times10^{-5}$
ϵ_5	$.812\times10^{-3}$	$-.126\times10^{-6}$	$-.751\times10^{-8}$	$.116\times10^{-9}$	$-.5\times10^{-9}$	$-.4\times10^{-7}$
No. of Points	1	10^3	10^3	10^2	10^6	10^6

VI

the h functions at 50 MeV

1(d)	1(e)	1(f)	1(g)	1(h)	1(i)	1(j)
$-.20\times10^{1}$	$-.53\times10^{-2}$	$.11\times10^{-1}$	$.32\times10^{-2}$	$.15\times10^{-2}$	$-.14\times10^{-1}$	$-.39\times10^{-1}$
$-.65\times10^{-1}$	$.44\times10^{-3}$	—	$-.12\times10^{-2}$	$.29\times10^{-3}$	$.95\times10^{-3}$	$-.15\times10^{-2}$
$-.68\times10^{-1}$	—	—	$-.97\times10^{-4}$	$-.32\times10^{-3}$	$-.20\times10^{-3}$	$-.23\times10^{-2}$
$-.64\times10^{-1}$	—	—	$.51\times10^{-3}$	$-.49\times10^{-3}$	$-.45\times10^{-4}$	$-.12\times10^{-2}$
$-.20\times10^{1}$	—	—	$-.39\times10^{-3}$	$.44\times10^{-3}$	$-.41\times10^{-2}$	$-.82\times10^{-1}$
$-.53\times10^{-2}$	—	—	$-.14\times10^{-5}$	$-.19\times10^{-5}$	$-.15\times10^{-4}$	$-.19\times10^{-3}$
$.20\times10^{-2}$	—	—	$.13\times10^{-3}$	$.38\times10^{-3}$	$-.29\times10^{-4}$	$.13\times10^{-3}$
$-.55\times10^{-2}$	—	—	$-.31\times10^{-5}$	$.17\times10^{-5}$	$-.81\times10^{-4}$	$-.85\times10^{-4}$
$-.54\times10^{-2}$	—	—	$.19\times10^{-5}$	$.33\times10^{-5}$	$-.19\times10^{-4}$	$-.18\times10^{-3}$
$-.78\times10^{-1}$	—	—	$-.83\times10^{-5}$	$-.13\times10^{-4}$	$-.11\times10^{-2}$	$-.11\times10^{-2}$
$-.5\times10^{-3}$	—	—	$-.6\times10^{-7}$	$.4\times10^{-7}$	$-.78\times10^{-5}$	$-.96\times10^{-5}$
$.6\times10^{-4}$	—	—	$.36\times10^{-5}$	$-.24\times10^{-5}$	$-.1\times10^{-5}$	$-.8\times10^{-6}$
$-.6\times10^{-3}$	—	—	$-.5\times10^{-7}$	$-.8\times10^{-7}$	$-.2\times10^{-5}$	$-.21\times10^{-4}$
$-.6\times10^{-3}$	—	—	$.15\times10^{-6}$	$-.1\times10^{-6}$	$-.88\times10^{-5}$	$-.97\times10^{-5}$
$-.6\times10^{-2}$	—	—	$.3\times10^{-7}$	$-.2\times10^{-6}$	$-.26\times10^{-4}$	$-.19\times10^{-3}$
$-.7\times10^{-4}$	—	—	$-.8\times10^{-9}$	$-.1\times10^{-8}$	$-.3\times10^{-6}$	$-.27\times10^{-5}$
$-.4\times10^{-5}$	—	—	$.5\times10^{-7}$	$.1\times10^{-6}$	$-.1\times10^{-7}$	$.1\times10^{-6}$
$-.7\times10^{-4}$	—	—	$-.5\times10^{-8}$	$.3\times10^{-8}$	$-.1\times10^{-5}$	$-.1\times10^{-5}$
$-.7\times10^{-4}$	—	—	$.3\times10^{-8}$	$.5\times10^{-8}$	$-.3\times10^{-6}$	$-.3\times10^{-5}$
$-.6\times10^{-3}$	—	—	$.3\times10^{-9}$	$.1\times10^{-8}$	$-.1\times10^{-4}$	$-.1\times10^{-4}$
$-.9\times10^{-5}$	—	—	$-.8\times10^{-10}$	$.5\times10^{-10}$	$-.1\times10^{-6}$	$-.2\times10^{-6}$
$-.4\times10^{-6}$	—	—	$.6\times10^{-8}$	$-.4\times10^{-8}$	$-.3\times10^{-8}$	$.4\times10^{-8}$
$-.9\times10^{-5}$	—	—	$-.1\times10^{-9}$	$-.2\times10^{-9}$	$-.4\times10^{-7}$	$-.4\times10^{-6}$
$-.9\times10^{-5}$	—	—	$.4\times10^{-9}$	$-.2\times10^{-9}$	$-.1\times10^{-6}$	$-.2\times10^{-6}$
$-.7\times10^{-4}$	—	—	$.1\times10^{-10}$	$-.1\times10^{-9}$	$-.3\times10^{-6}$	$-.3\times10^{-5}$
$-.1\times10^{-5}$	—	—	$-.2\times10^{-11}$	$-.3\times10^{-11}$	$-.5\times10^{-8}$	$-.6\times10^{-7}$
10^{6}	—	10^{7}	10^{5}	10^{5}	10^{5}	10^{5}

TABLE

Values of the real parts of

	OPE	BOX	X-BOX	1(a)	1(b)	1(c)
$^1S_0$	$-.947\times10^{-1}$	$.250\times10^{-1}$	$.322\times10^{-1}$	$-.420\times10^{0}$	$-.50\times10^{0}$	$-.16\times10^{1}$
$^3P_0$	$.947\times10^{-1}$	$.530\times10^{-2}$	$-.499\times10^{-2}$	$-.259\times10^{-1}$	$.70\times10^{-1}$	$-.42\times10^{-1}$
$^1P_1$	$-.331\times10^{-1}$	$.309\times10^{-2}$	$-.177\times10^{-2}$	$-.331\times10^{-1}$	$.61\times10^{-1}$	$-.98\times10^{-1}$
$^3P_1$	$-.529\times10^{-1}$	$.169\times10^{-2}$	$.800\times10^{-3}$	$-.295\times10^{-1}$	$.65\times10^{-1}$	$-.76\times10^{-1}$
$^3S_1$	$-.947\times10^{-1}$	$.190\times10^{0}$	$-.235\times10^{-1}$	$-.420\times10^{0}$	$-.50\times10^{0}$	$-.16\times10^{1}$
$^3D_1$	$-.308\times10^{-1}$	$-.229\times10^{-2}$	$-.615\times10^{-4}$	$-.422\times10^{-2}$	$.13\times10^{-1}$	$-.99\times10^{-2}$
ϵ_1	$.904\times10^{-1}$	$-.508\times10^{-2}$	$-.733\times10^{-3}$	$.220\times10^{-4}$	$.3\times10^{-4}$	$-.38\times10^{-2}$
$^1D_2$	$.476\times10^{-2}$	$.570\times10^{-4}$	$.336\times10^{-3}$	$-.472\times10^{-2}$	$.14\times10^{-1}$	$-.13\times10^{-1}$
$^3D_2$	$.404\times10^{-1}$	$.106\times10^{-2}$	$-.146\times10^{-3}$	$-.453\times10^{-2}$	$.14\times10^{-1}$	$-.12\times10^{-1}$
$^3P_2$	$.617\times10^{-2}$	$.899\times10^{-3}$	$.203\times10^{-2}$	$-.367\times10^{-1}$	$.56\times10^{-1}$	$-.11\times10^{0}$
$^3F_2$	$.253\times10^{-2}$	$-.176\times10^{-4}$	$.295\times10^{-4}$	$-.751\times10^{-3}$	$.28\times10^{-2}$	$-.18\times10^{-2}$
ϵ_2	$-.892\times10^{-2}$	$-.258\times10^{-4}$	$.430\times10^{-4}$	$.119\times10^{-5}$	$-.2\times10^{-5}$	$-.2\times10^{-3}$
$^1F_3$	$-.657\times10^{-2}$	$.880\times10^{-4}$	$-.317\times10^{-4}$	$-.818\times10^{-3}$	$.3\times10^{-2}$	$-.2\times10^{-2}$
$^3F_3$	$-.480\times10^{-2}$	$.161\times10^{-4}$	$.442\times10^{-4}$	$-.800\times10^{-3}$	$.3\times10^{-2}$	$-.2\times10^{-2}$
$^3D_3$	$-.542\times10^{-2}$	$.896\times10^{-3}$	$-.183\times10^{-3}$	$-.509\times10^{-2}$	$.14\times10^{-1}$	$-.14\times10^{-1}$
$^3G_3$	$-.242\times10^{-2}$	$-.160\times10^{-4}$	$-.375\times10^{-5}$	$-.148\times10^{-3}$	$.6\times10^{-3}$	$-.3\times10^{-3}$
ϵ_3	$.104\times10^{-1}$	$-.260\times10^{-4}$	$-.283\times10^{-5}$	$.118\times10^{-6}$	$-.3\times10^{-6}$	$-.2\times10^{-4}$
$^1G_4$	$.104\times10^{-2}$	$.188\times10^{-5}$	$.964\times10^{-5}$	$-.159\times10^{-3}$	$.7\times10^{-3}$	$-.4\times10^{-3}$
$^3G_4$	$.589\times10^{-2}$	$.256\times10^{-4}$	$-.502\times10^{-5}$	$-.157\times10^{-3}$	$.6\times10^{-2}$	$-.4\times10^{-3}$
$^3F_4$	$.627\times10^{-3}$	$.154\times10^{-4}$	$.493\times10^{-4}$	$-.873\times10^{-3}$	$.3\times10^{-2}$	$-.2\times10^{-2}$
$^3H_4$	$.293\times10^{-3}$	$-.196\times10^{-6}$	$.133\times10^{-5}$	$-.314\times10^{-4}$	$.1\times10^{-3}$	$-.7\times10^{-4}$
ϵ_4	$-.149\times10^{-2}$	$-.453\times10^{-6}$	$.696\times10^{-6}$	$.157\times10^{-7}$	$-.6\times10^{-7}$	$-.3\times10^{-5}$
$^1H_5$	$-.152\times10^{-2}$	$.353\times10^{-5}$	$-.116\times10^{-5}$	$-.336\times10^{-4}$	$.1\times10^{-3}$	$-.8\times10^{-4}$
$^3H_5$	$-.863\times10^{-3}$	$.568\times10^{-6}$	$.170\times10^{-5}$	$-.332\times10^{-4}$	$.1\times10^{-3}$	$-.8\times10^{-4}$
$^3G_5$	$-.719\times10^{-3}$	$.252\times10^{-4}$	$-.549\times10^{-5}$	$-.169\times10^{-3}$	$.7\times10^{-3}$	$-.4\times10^{-3}$
$^3I_5$	$-.345\times10^{-3}$	$-.167\times10^{-6}$	$-.175\times10^{-6}$	$-.758\times10^{-5}$	$.3\times10^{-4}$	$-.2\times10^{-4}$
ϵ_5	$.205\times10^{-2}$	$-.756\times10^{-6}$	$-.734\times10^{-7}$	$.247\times10^{-8}$	$-.1\times10^{-7}$	$-.4\times10^{-6}$
No. of Points	1	10^3	10^3	10^2	10^6	10^6

VII

the h functions at 100 MeV.

1(d)	1(e)	1(f)	1(g)	1(h)	1(i)	1(j)
$-.18\times10^{1}$	$-.50\times10^{-2}$	9.5×10^{-2}	$.38\times10^{-2}$	$.92\times10^{-3}$	$-.11\times10^{-1}$	$-.37\times10^{-1}$
$-.96\times10^{-1}$	$.68\times10^{-3}$	—	$-.23\times10^{-2}$	$.53\times10^{-3}$	$.24\times10^{-2}$	$-.24\times10^{-2}$
$-.10\times10^{0}$	—	—	$-.18\times10^{-3}$	$-.62\times10^{-3}$	$-.23\times10^{-3}$	$-.33\times10^{-2}$
$-.93\times10^{-1}$	—	—	$.98\times10^{-3}$	$-.94\times10^{-3}$	$.46\times10^{-3}$	$-.18\times10^{-2}$
$-.18\times10^{1}$	—	—	$-.42\times10^{-3}$	$.97\times10^{-4}$	$-.34\times10^{-2}$	$-.79\times10^{-1}$
$-.12\times10^{-1}$	—	—	$-.5\times10^{-5}$	$-.6\times10^{-5}$	$-.2\times10^{-4}$	$-.38\times10^{-3}$
$.37\times10^{-2}$	—	—	$.25\times10^{-3}$	$.74\times10^{-3}$	$-.5\times10^{-4}$	$.26\times10^{-3}$
$-.13\times10^{-1}$	—	—	$-.1\times10^{-4}$	$.5\times10^{-5}$	$-.16\times10^{-3}$	$-.17\times10^{-3}$
$-.13\times10^{-1}$	—	—	$.6\times10^{-5}$	$.1\times10^{-4}$	$-.4\times10^{-4}$	$-.37\times10^{-3}$
$-.12\times10^{0}$	—	—	$-.2\times10^{-4}$	$-.3\times10^{-4}$	$-.16\times10^{-2}$	$-.16\times10^{-2}$
$-.20\times10^{-2}$	—	—	$-.3\times10^{-6}$	$.2\times10^{-6}$	$-.2\times10^{-4}$	$-.3\times10^{-4}$
$.2\times10^{-3}$	—	—	$.1\times10^{-4}$	$-.8\times10^{-5}$	$-.4\times10^{-5}$	$.2\times10^{-5}$
$-.2\times10^{-2}$	—	—	$-.3\times10^{-6}$	$-.5\times10^{-6}$	$-.8\times10^{-5}$	$-.6\times10^{-4}$
$-.2\times10^{-2}$	—	—	$.9\times10^{-6}$	$-.6\times10^{-6}$	$-.3\times10^{-4}$	$-.3\times10^{-4}$
$-.14\times10^{-1}$	—	—	$.8\times10^{-7}$	$-.8\times10^{-6}$	$-.6\times10^{-4}$	$-.38\times10^{-3}$
$-.4\times10^{-3}$	—	—	$-.8\times10^{-8}$	$-.1\times10^{-7}$	$-.1\times10^{-5}$	$-.1\times10^{-4}$
$.2\times10^{-4}$	—	—	$.3\times10^{-6}$	$.6\times10^{-6}$	$-.5\times10^{-7}$	$.3\times10^{-6}$
$-.4\times10^{-3}$	—	—	$-.5\times10^{-7}$	$.3\times10^{-7}$	$-.6\times10^{-5}$	$-.5\times10^{-5}$
$-.4\times10^{-3}$	—	—	$.3\times10^{-7}$	$.5\times10^{-7}$	$-.2\times10^{-5}$	$-.1\times10^{-4}$
$-.2\times10^{-2}$	—	—	$-.4\times10^{-8}$	$.1\times10^{-7}$	$-.3\times10^{-4}$	$-.3\times10^{-4}$
$-.8\times10^{-4}$	—	—	$-.1\times10^{-8}$	$.9\times10^{-9}$	$-.1\times10^{-5}$	$-.1\times10^{-5}$
$.3\times10^{-5}$	—	—	$.5\times10^{-7}$	$-.4\times10^{-7}$	$-.2\times10^{-7}$	$.2\times10^{-7}$
$-.8\times10^{-4}$	—	—	$-.2\times10^{-8}$	$-.4\times10^{-8}$	$-.3\times10^{-6}$	$-.2\times10^{-5}$
$-.8\times10^{-4}$	—	—	$.6\times10^{-8}$	$-.4\times10^{-8}$	$-.1\times10^{-5}$	$-.1\times10^{-5}$
$-.4\times10^{-3}$	—	—	$-.6\times10^{-10}$	$-.1\times10^{-8}$	$-.2\times10^{-5}$	$-.1\times10^{-4}$
$-.2\times10^{-4}$	—	—	$-.5\times10^{-10}$	$-.9\times10^{-10}$	$-.6\times10^{-7}$	$-.5\times10^{-6}$
$.4\times10^{-6}$	—	—	$.2\times10^{-8}$	$.4\times10^{-8}$	$-.6\times10^{-9}$	$.6\times10^{-8}$
10^{6}	—	10^{7}	10^{5}	10^{5}	10^{5}	10^{5}

TABLE

Values of the real parts of

	OP	BOX	X-BOX	1(a)	1(b)	1(c)
$^1S_0$	$-.106\times10^{0}$	$.244\times10^{-1}$	$.248\times10^{-1}$	$-.360\times10^{0}$	$-.58\times10^{0}$	$-.14\times10^{1}$
$^3P_0$	$.106\times10^{0}$	$.683\times10^{-2}$	$-.997\times10^{-2}$	$-.297\times10^{-1}$	$.79\times10^{-1}$	$-.31\times10^{-1}$
$^1P_1$	$-.255\times10^{-1}$	$.345\times10^{-2}$	$-.238\times10^{-2}$	$-.416\times10^{-1}$	$.59\times10^{-1}$	$-.13\times10^{0}$
$^3P_1$	$-.571\times10^{-1}$	$.206\times10^{-2}$	$.276\times10^{-3}$	$-.356\times10^{-1}$	$.69\times10^{-1}$	$-.90\times10^{-1}$
$^3S_1$	$-.106\times10^{0}$	$.175\times10^{0}$	$-.223\times10^{-1}$	$-.360\times10^{0}$	$-.58\times10^{0}$	$-.14\times10^{1}$
$^3D_1$	$-.402\times10^{-1}$	$-.490\times10^{-2}$	$-.364\times10^{-4}$	$-.745\times10^{-2}$	$.20\times10^{-1}$	$-.17\times10^{-1}$
ϵ_1	$.928\times10^{-1}$	$-.603\times10^{-2}$	$-.131\times10^{-2}$	$.709\times10^{-4}$	$.1\times10^{-3}$	$-.66\times10^{-2}$
$^1D_2$	$.441\times10^{-2}$	$.102\times10^{-3}$	$.644\times10^{-3}$	$-.863\times10^{-2}$	$.21\times10^{-1}$	$-.24\times10^{-1}$
$^3D_2$	$.490\times10^{-1}$	$.173\times10^{-2}$	$-.246\times10^{-3}$	$-.817\times10^{-2}$	$.21\times10^{-1}$	$-.22\times10^{-1}$
$^3P_2$	$.803\times10^{-2}$	$.121\times10^{-2}$	$.254\times10^{-2}$	$-.475\times10^{-1}$	$.49\times10^{-1}$	$-.15\times10^{0}$
$^3F_2$	$.388\times10^{-2}$	$-.536\times10^{-4}$	$.640\times10^{-4}$	$-.191\times10^{-2}$	$.62\times10^{-2}$	$-.45\times10^{-2}$
ϵ_2	$-.102\times10^{-1}$	$-.344\times10^{-4}$	$.106\times10^{-3}$	$.573\times10^{-5}$	$-.5\times10^{-5}$	$-.5\times10^{-3}$
$^1F_3$	$-.732\times10^{-2}$	$.223\times10^{-3}$	$-.871\times10^{-4}$	$-.214\times10^{-2}$	$.68\times10^{-2}$	$-.56\times10^{-2}$
$^3F_3$	$-.668\times10^{-2}$	$.360\times10^{-4}$	$.116\times10^{-3}$	$-.208\times10^{-2}$	$.66\times10^{-2}$	$-.52\times10^{-2}$
$^3D_3$	$-.832\times10^{-2}$	$.171\times10^{-2}$	$-.364\times10^{-3}$	$-.955\times10^{-2}$	$.22\times10^{-1}$	$-.27\times10^{-1}$
$^3G_3$	$-.441\times10^{-2}$	$-.739\times10^{-4}$	$-.127\times10^{-4}$	$-.535\times10^{-3}$	$.20\times10^{-2}$	$-.12\times10^{-2}$
ϵ_2	$.135\times10^{-1}$	$-.427\times10^{-4}$	$-.989\times10^{-5}$	$.817\times10^{-6}$	$-.2\times10^{-5}$	$-.7\times10^{-4}$
$^1G_4$	$.140\times10^{-2}$	$.664\times10^{-5}$	$.375\times10^{-4}$	$-.591\times10^{-3}$	$.2\times10^{-2}$	$-.1\times10^{-2}$
$^3G_4$	$.953\times10^{-2}$	$.793\times10^{-4}$	$-.190\times10^{-4}$	$-.579\times10^{-3}$	$.2\times10^{-2}$	$-.1\times10^{-2}$
$^3F_4$	$.114\times10^{-2}$	$.412\times10^{-4}$	$.139\times10^{-3}$	$-.234\times10^{-2}$	$.7\times10^{-2}$	$-.6\times10^{-2}$
$^3H_4$	$.636\times10^{-3}$	$-.156\times10^{-5}$	$.661\times10^{-5}$	$-.160\times10^{-3}$	$.6\times10^{-3}$	$-.4\times10^{-3}$
ϵ_4	$-.227\times10^{-2}$	$-.973\times10^{-6}$	$.336\times10^{-5}$	$.154\times10^{-6}$	$-.5\times10^{-6}$	$-.1\times10^{-4}$
$^1H_5$	$-.245\times10^{-2}$	$.172\times10^{-4}$	$-.633\times10^{-5}$	$-.175\times10^{-3}$	$.7\times10^{-3}$	$-.4\times10^{-3}$
$^3H_5$	$-.163\times10^{-2}$	$.244\times10^{-5}$	$.914\times10^{-5}$	$-.172\times10^{-3}$	$.7\times10^{-3}$	$-.4\times10^{-3}$
$^3G_5$	$-.156\times10^{-2}$	$.941\times10^{-4}$	$-.219\times10^{-4}$	$-.640\times10^{-3}$	$.2\times10^{-2}$	$-.2\times10^{-2}$
$^3I_5$	$-.893\times10^{-3}$	$-.301\times10^{-5}$	$-.125\times10^{-5}$	$-.506\times10^{-4}$	$.2\times10^{-3}$	$-.1\times10^{-3}$
ϵ_5	$.366\times10^{-2}$	$-.220\times10^{-5}$	$-.490\times10^{-6}$	$.342\times10^{-7}$	$-.1\times10^{-6}$	$-.3\times10^{-5}$
No. of Points	1	10^3	10^3	10^2	10^6	10^6

VIII

the h functions at 200 MeV.

1(d)	1(e)	1(f)	1(g)	1(h)	1(i)	1(j)
$-.16\times10^{1}$	$-.46\times10^{-2}$	9.5×10^{-2}	$.49\times10^{-2}$	$-.14\times10^{-3}$	$-.71\times10^{-2}$	$-.34\times10^{-1}$
$-.12\times10^{0}$	$.11\times10^{-2}$	—	$-.45\times10^{-2}$	$.95\times10^{-3}$	$.53\times10^{-2}$	$-.38\times10^{-2}$
$-.13\times10^{0}$	—	—	$-.35\times10^{-3}$	$-.12\times10^{-2}$	$-.20\times10^{-3}$	$-.45\times10^{-2}$
$-.12\times10^{0}$	—	—	$.19\times10^{-2}$	$-.18\times10^{-2}$	$.17\times10^{-2}$	$-.26\times10^{-2}$
$-.16\times10^{1}$	—	—	$-.47\times10^{-3}$	$-.60\times10^{-3}$	$-.25\times10^{-2}$	$-.71\times10^{-1}$
$-.24\times10^{-1}$	—	—	$-.16\times10^{-4}$	$-.18\times10^{-4}$	$-.19\times10^{-4}$	$-.77\times10^{-3}$
$.65\times10^{-2}$	—	—	$.47\times10^{-3}$	$.14\times10^{-2}$	$-.99\times10^{-4}$	$.46\times10^{-3}$
$-.25\times10^{-1}$	—	—	$-.29\times10^{-4}$	$.13\times10^{-4}$	$-.29\times10^{-3}$	$-.34\times10^{-3}$
$-.24\times10^{-1}$	—	—	$.19\times10^{-4}$	$.29\times10^{-4}$	$-.55\times10^{-4}$	$-.74\times10^{-3}$
$-.16\times10^{0}$	—	—	$-.46\times10^{-4}$	$-.51\times10^{-4}$	$-.22\times10^{-2}$	$-.21\times10^{-2}$
$-.54\times10^{-2}$	—	—	$-.2\times10^{-5}$	$.1\times10^{-5}$	$-.52\times10^{-4}$	$-.7\times10^{-4}$
$.5\times10^{-3}$	—	—	$.34\times10^{-4}$	$-.22\times10^{-4}$	$-.1\times10^{-4}$	$.6\times10^{-5}$
$-.57\times10^{-2}$	—	—	$-.1\times10^{-5}$	$-.2\times10^{-5}$	$-.22\times10^{-4}$	$-.16\times10^{-3}$
$-.56\times10^{-2}$	—	—	$.4\times10^{-5}$	$-.3\times10^{-5}$	$-.7\times10^{-4}$	$-.7\times10^{-4}$
$-.28\times10^{-1}$	—	—	$.2\times10^{-6}$	$-.3\times10^{-5}$	$-.11\times10^{-3}$	$-.74\times10^{-3}$
$-.14\times10^{-2}$	—	—	$-.7\times10^{-7}$	$-.1\times10^{-6}$	$-.5\times10^{-5}$	$-.4\times10^{-4}$
$.7\times10^{-4}$	—	—	$.1\times10^{-5}$	$.3\times10^{-5}$	$-.3\times10^{-6}$	$.1\times10^{-5}$
$-.1\times10^{-2}$	—	—	$-.4\times10^{-6}$	$.2\times10^{-6}$	$-.2\times10^{-4}$	$-.2\times10^{-4}$
$-.1\times10^{-2}$	—	—	$.2\times10^{-6}$	$.4\times10^{-6}$	$-.6\times10^{-5}$	$-.4\times10^{-4}$
$-.6\times10^{-2}$	—	—	$-.6\times10^{-7}$	$.6\times10^{-7}$	$-.1\times10^{-3}$	$-.8\times10^{-4}$
$-.4\times10^{-3}$	—	—	$-.2\times10^{-7}$	$.1\times10^{-7}$	$-.5\times10^{-5}$	$-.5\times10^{-5}$
$.1\times10^{-4}$	—	—	$.4\times10^{-6}$	$-.3\times10^{-6}$	$-.1\times10^{-6}$	$.1\times10^{-6}$
$-.4\times10^{-3}$	—	—	$-.2\times10^{-7}$	$-.4\times10^{-7}$	$-.2\times10^{-5}$	$-.1\times10^{-4}$
$-.4\times10^{-3}$	—	—	$.7\times10^{-7}$	$-.5\times10^{-7}$	$-.6\times10^{-5}$	$-.6\times10^{-5}$
$-.2\times10^{-2}$	—	—	$-.2\times10^{-8}$	$-.2\times10^{-7}$	$-.7\times10^{-6}$	$-.4\times10^{-4}$
$-.1\times10^{-3}$	—	—	$-.1\times10^{-8}$	$-.2\times10^{-8}$	$-.5\times10^{-6}$	$-.4\times10^{-5}$
$.3\times10^{-5}$	—	—	$.3\times10^{-7}$	$.5\times10^{-7}$	$-.7\times10^{-8}$	$.5\times10^{-7}$
10^{6}		10^{7}	10^{5}	10^{5}	10^{5}	10^{5}

such that $g^2 = 14$; that is, $g^2/4\pi$ (reference 18) $= g^2$ (present work). The factor connecting the two expansions is

$$Re\, h_0(^1S_0) = \frac{E}{2mp} \tan \delta(^1S_0).$$

In higher orders, this last equation has to be modified to take account of the fact that

$$\begin{aligned} h_0(^1S_0) &= \frac{E}{2mp} \operatorname{Re} \left[\frac{\exp(2i\delta(^1S_0)) - 1}{2i}\right]. \\ &= \frac{E}{2mp} \sin \delta(^1S_0) \cos \delta(^1S_0) \\ &= \frac{E}{2mp} \frac{\tan \delta(^1S_0)}{1 + \tan^2 \delta(^1S_0)} \\ &= \frac{E}{2mp} \left[\tan (^1S_0) - \tan^3 (^1S_0) + \cdots\right]. \end{aligned}$$

It must be remembered that the 2 in $E/2mp$ occurs because the Pauli principle factor 2 has not been included in Tables VI–VIII.

Using $E = \sqrt{p^2 + m^2}$, $(p/m)^2 = E_{LAB}/2m$, we find for $E_{LAB} = 100$ MeV,

$$(p/m)^2 = \frac{100 \text{ MeV}}{2(940) \text{ MeV}} = 0.05319,$$

so that in units such that $m = 1$,

$$\frac{E}{2mp} = \frac{\sqrt{p^2 + m^2}}{2mp} = \frac{\sqrt{1.05319}}{2\sqrt{0.05319}} = 2.225,$$

which agrees with the ratios (0.0947/0.04263) and (0.0250/0.0126).

The entries such as $^1S_0$, $^3S_1$, $^3D_1$, 2_1, in Tables VI–VIII, refer to the real parts of h_0, $h_{0,1}$, $h_{2,1}$, h^1, respectively, in an obvious way, and similarly for other quantities.

No effort has been made to give error estimates for the individual numbers; however, only significant figures are given so that the relative precision is easily noted. For purposes of comparison, the second- and fourth-order results are presented. The Pauli principle has been ignored and all graphs are taken with $g^2 = \lambda = 1$. All isospin factors and multiplicities have been included. To find the relative sizes of the perturbation terms, one must note that $g^2 \approx 14$ and that, although λ is not well determined, a calculation which fits the ρ resonance [7] uses $\lambda \approx 0.1$.

IV. Conclusions about Techniques

In order to estimate the effects of some higher-order graphs on NN scattering from perturbation theory, we have computed sixth-order graphs with pion exchange as well as some graphs with a $\lambda\phi^4$ interaction. We have used various techniques to evaluate these amplitudes. Monte Carlo integration has been employed in a modified form to deal with integrands that are not smooth along with an extrapolation $s + i\epsilon \to s + i0^+$ for singular integrals. In addition, we have used changes of variable suited to allow handling some integrable boundary singularities.

It is found that computation of the sixth-order contributions is rather difficult, especially in the case of graphs which contain the unitary cut. For the ladder graph our methods have proved inadequate so we can only take some limited results from the Bethe–Salpeter calculation [18, 20]. The other singular graph of Fig. 1(f) is somewhat better in that we can find the full amplitude to within about 10% using the $\epsilon \to 0$ extrapolation. Still this allows us only to find the lower partial waves. For this graph, the procedure used for averaging pairs of contributions on opposite sides of the singular surface proved to be quite useful in improving the rate of convergence. The remaining nonsingular sixth-order graphs were evaluated using the method of dividing the region up into hypercubes and dealing with them individually. In these cases the full amplitudes have been found with a precision of roughly 1% which allows a partial-wave projection with marginal accuracy.

The amplitudes of order $g^4\lambda^2$ have been evaluated to an accuracy of about 1%. The chief difficulties with these amplitudes are the integrable boundary singularities. These have been handled by an appropriate change of variable which sufficiently weakens the singularities that the integrals can be carried out by Monte Carlo methods.

V. Discussion of Results from a Conventional Viewpoint

The contributions to the various partial waves to the real part of the scattering amplitude (Tables VI–VIII) of the graphs of Figs. 1(f–h), which are the three meson exchange graphs, confirm that these contributions decrease more rapidly than those of the two-pion exchange graphs (the fourth-order graphs and the graphs of Figs. 1(i) and (j)).

Machida and Ueda [21] and Klein[11] and others [9, 10] calculated three meson exchange contributions in terms of potentials. They found that the three-meson exchange terms decrease more rapidly with distance than the two-meson exchange

terms, so that the above result had to be expected. This whole idea about decrease of multiple pion exchanges with increasing L came to fruition when it was found that the one-pion exchange terms dominate the higher partial waves [2, 12]. Since then, many attempts have been made to explain the medium partial waves by considering two-pion exchange and including exchange of more massive bosons [22–26].

Comparing the contributions of Figs. 1(i) and (j) with those of the fourth-order graphs, it is apparent that they decrease with angular momentum at the same rate, as expected. The sixth-order contributions are comparable to or larger than the fourth-order contributions. The fears of Partovi and Lomon [26] on this point appear quite justified. This is very nearly the result suggested by the early work of Lévy [9], Ruderman [10], and Klein [11] based on an approximation which was used to generate potentials from such sixth order graphs. However, the sum of the radiative corrections on one nucleon line give rise to the pion–nucleon scattering amplitude [27], and Henley and Ruderman [28] have shown that higher order corrections suppress the sixth-order result. Here phenomenological approaches such as somehow inserting the pion–nucleon amplitude in two-pion exchange graphs obviously suggest themselves, but the accuracy of such approaches, which amount to summation of certain classes of diagrams, is not known and is quite foreign to the idea that the whole series may be summed by Padé approximants.

It has already been noted by Anderson, *et al.* [17] that the graph of order λg^4 behaves very much like exchange of a single scalar particle. For the graphs of order $\lambda^2 g^4$ we note that they fall off with angular momentum at a rate between that of one-pion exchange and two-pion exchange and they give mostly a spin–orbit type contribution to the P-wave splitting.

Appendix

For reference purposes we will give in this appendix a fairly complete set of relationships among this various amplitudes encountered earlier.

The invariant amplitude F is related to the S matrix element according to the following:

$$S = 1 + i(2\pi)^4 \, \delta \left(\sum p_i - \sum p_f \right) N_1 N_2 N_3 N_4 F, \tag{A1}$$

where $N_i = \{[1/(2\pi)^3](m_i/E_i)\}^{1/2}$.

Now F can be decomposed in many ways. Amati *et al.* [15] have written F in terms of perturbation invariants as

$$\begin{aligned} F = {} & A_1[(1)_1\,(1)_2] \\ & + A_2[(1)_1\,(i\gamma\cdot p_1)_2 + (i\gamma\cdot p_2)_1\,(1)_2] \\ & + A_3[(i\gamma\cdot p_2)_1\,(i\gamma\cdot p_1)_2] \\ & + A_4[(\gamma_\mu)_1\,(\gamma_\mu)_2] \\ & + A_5[(\gamma_5)_1\,(\gamma_5)_2] \\ = {} & \sum_{i=1}^{5} A_i P_i\,. \end{aligned} \tag{A2}$$

The notation $(X)_i$ indicates $\bar{u}(p_i')[X]\,u(p_i)$, and the A_i are scalar functions of s, t, and u.

Goldberger *et al.* [16] have introduced the reduction

$$F = F_1(S-\tilde{S}) + F_2(T+\tilde{T}) + F_3(A-\tilde{A}) + F_4(V+\tilde{V}) + F_5(P-\tilde{P}). \tag{A3}$$

Here F_i are scalar functions and

$$\begin{aligned} S &= (1)_1\,(1)_2\,, \\ T &= \tfrac{1}{2}(i\gamma_\mu\gamma_\nu)_1\,(i\gamma_\mu\gamma_\nu)_2\,, \\ A &= (i\gamma_5\gamma_\mu)_1\,(i\gamma_5\gamma_\mu)_2\,, \\ V &= (\gamma_\mu)_1\,(\gamma_\mu)_2\,, \end{aligned} \tag{A4}$$

and

$$P = (\gamma_5)_1\,(\gamma_5)_2\,.$$

The corresponding quantities with tildes are found by interchanging p_1' and p_2' in the spinor arguments. The necessary information relating the quantities with tildes to the others is given in the following matrix:

$$\begin{bmatrix} S \\ V \\ T \\ A \\ P \end{bmatrix} = \tfrac{1}{4} \begin{bmatrix} 2 & 1 & 1 & 0 & 0 \\ -4 & 2 & 0 & -2 & 4 \\ -6 & 0 & 2 & 0 & -6 \\ 0 & 2 & 0 & 2 & 0 \\ 0 & -1 & 1 & 0 & 2 \end{bmatrix} \begin{bmatrix} S-\tilde{S} \\ V+\tilde{V} \\ T+\tilde{T} \\ A-\tilde{A} \\ P-\tilde{P} \end{bmatrix}. \tag{A5}$$

The relationships among the P_i and the S, T, etc., amplitudes has been given by Amati *et al.* [15] as

$$\begin{aligned} P_1 &= S, \\ P_2 &= \frac{1}{m}\left[\frac{(u-s)}{4} S - m^2 V + \frac{tT}{4} + \frac{(u-s)}{4} P\right], \\ P_3 &= \tfrac{1}{4}\left[-(u-s)\, V - tA + 4m^2 P\right], \\ P_4 &= V, \\ P_5 &= P. \end{aligned} \tag{A6}$$

The nuclear-bar phase shifts can be written as combinations of the projections of the five invariant scalar functions F_i. Using the notation of Scotti and Wong [19] the phase shifts are given in terms of the h functions by

$$\begin{aligned} h_J &= (E/2imp)(\exp(2i\delta_J) - 1), \\ h_{JJ} &= (E/2imp)(\exp(2i\delta_{JJ}) - 1), \\ h_{J-1,J} &= (E/2imp)(\cos(2\epsilon_J)\exp(2i\delta_{J-1,J}) - 1), \\ h_{J+1,J} &= (E/2imp)(\cos(2\epsilon_J)\exp(2i\delta_{J+1,J}) - 1), \end{aligned} \tag{A7}$$

and

$$h^J = (E/2imp)\sin(2\epsilon_J)\exp(i\delta_{J-1,J} + i\delta_{J+1,J}).$$

Here E and p are the center-of-mass energy and momentum of one of the particles of mass m. The h functions in terms of the Legendre projections of the F_i are now

$$\begin{aligned} 8\pi m h_J = {} & (E^2 + m^2) F_1{}^J - \frac{2p^2}{2J+1}\left((J+1) F_2^{J+1} + J F_2^{J-1}\right) \\ & - (4E^2 + 2m^2) F_3{}^J + p^2 F_5{}^J, \\ 8\pi m h_{JJ} = {} & -\frac{p^2}{2J+1}\left(J F_1^{J+1} + (J+1) F_1^{J-1}\right) + 2m^2 F_2{}^J \\ & + \frac{2p^2}{2J+1}\left(J F_3^{J+1} + (J+1) F_3^{J-1}\right) + 2E^2 F_4{}^J \\ & + \frac{p^2}{2J+1}\left(J F_5^{J+1} + (J+1) F_5^{J-1}\right), \end{aligned}$$

$$
\begin{aligned}
8\pi m h_{J-1,J} = & -p^2 F_1^J + \frac{2J(J+1)}{(2J+1)^2}(E-m)^2 F_2^{J+1} \\
& + \frac{2}{(2J+1)^2}(JE+(J+1)m)^2 F_2^{J-1} - \frac{2(J-1)}{2J+1} p^2 F_3^J \\
& + \frac{2J(J+1)}{(2J+1)^2}(E-m)^2 F_4^{J+1} + \frac{2}{(2J+1)^2}(mJ+E(J+1))^2 F_4^{J-1} \\
& + \frac{p^2}{2J+1} F_5^J,
\end{aligned} \tag{A8}
$$

$$
\begin{aligned}
8\pi m h_{J+1,J} = & -p^2 F_1^J + \frac{2J(J+1)}{(2J+1)^2}(E-m)^2 F_2^{J-1} \\
& + \frac{2}{(2J+1)^2}((J+1)E+Jm)^2 F_2^{J+1} - \frac{2p^2}{2J+1}(J+2) F_3^J \\
& + \frac{2J(J+1)}{(2J+1)^2}(E-m)^2 F_4^{J-1} + \frac{2}{(2J+1)^2}((J+1)m+JE)^2 F_4^{J+1} \\
& - \frac{p^2}{2J+1} F_5^J,
\end{aligned}
$$

and

$$
\begin{aligned}
8\pi m h^J = & \left(\frac{J(J+1)}{(2J+1)^2}\right)^{1/2} \Big[\frac{2}{2J+1}(E^2(J+1) - m^2 J - mE) F_2^{J+1} \\
& + \frac{2}{2J+1}(JE^2 - m^2(J+1) + mE) F_2^{J-1} - 6p^2 F_3^J \\
& + \frac{2}{2J+1}(m^2(J+1) - E^2 J - mE) F_4^{J+1} \\
& + \frac{2}{2J+1}(m^2 J - E^2(J+1) + mE) F_4^{J-1} - 2p^2 F_5^J \Big].
\end{aligned}
$$

From the result of (27) it is clear that three types of terms occur which do not readily reduce to the standard form for NN amplitudes. These are

$$
\begin{aligned}
(\gamma_5\gamma_\mu)_1 (\gamma_5\gamma_\mu i\gamma \cdot p_1)_2 &\equiv Z_1, \\
(\gamma_5\gamma_\mu i\gamma \cdot p_2)_1 (\gamma_5\gamma_\mu)_2 &\equiv Z_2,
\end{aligned} \tag{A9}
$$

and

$$
(\gamma_5\gamma_\mu i\gamma \cdot p_2)_1 (\gamma_5\gamma_\mu i\gamma \cdot p_1)_2 \equiv Z.
$$

The method for reduction of these forms has been given in the text and it requires writing $\gamma_\mu\gamma_\mu$ in terms of components. The results are the following:

$$
\begin{aligned}
Z_1 = {} & m\left[\frac{-4m^2u - st}{su(s-4m^2)}\right] G + Q_2 + m\left[\frac{2(s-2m^2)}{t}\right] P_5 \\
& - m\left[\frac{s^2-u^2}{stu}\right] P_3 - m^2\left[\frac{(s-u)^2}{stu}\right] P_2{}^P \\
& - \left[\frac{(s+u)(m^2(s+u)-su)}{stu}\right] P_2{}^N \\
& - m\left[\frac{(s-u)(m^2(s+u)-su)}{stu}\right] P_1 , \\
Z_2 = {} & m\left[\frac{-4m^2u - st}{su(s-4m^2)}\right] G + Q_1 + m\left[\frac{2(s-2m^2)}{t}\right] P_5 \\
& - m\left[\frac{s^2-u^2}{stu}\right] P_3 - m^2\left[\frac{(s-u)^2}{stu}\right] P_2{}^N \\
& - \left[\frac{(s+u)(m^2(s+u)-su)}{stu}\right] P_2{}^P \\
& - m\left[\frac{(s-u)(m^2(s+u)-su)}{stu}\right] P_1 ,
\end{aligned}
\tag{A10}
$$

and

$$
\begin{aligned}
Z = {} & m^2\left[\frac{2u(s-2m^2)+st}{su(s-4m^2)}\right] G + mQ_1 + mQ_2 \\
& + \left[s - \frac{(s-2m^2)^2}{t}\right] P_5 + m^2\left[\frac{(s-u)^2}{stu}\right] P_3 \\
& + m\left[\frac{(s-u)(m^2(s+u)-su)}{stu}\right] P_2 + \left[\frac{(m^2(s+u)-su)^2}{stu}\right] P_1 .
\end{aligned}
$$

The quantities which appear are

$$
\begin{aligned}
Q_1 &= \tfrac{1}{2}(\gamma_5)_1\,(\gamma_5 i\gamma\cdot(p_1+p_1'))_2 , \\
Q_2 &= \tfrac{1}{2}(\gamma_5 i\gamma\cdot(p_2+p_2'))_1\,(\gamma_5)_2 , \\
G &= \tfrac{1}{4}(\gamma_5 i\gamma\cdot(p_2+p_2'))_1\,(\gamma_5 i\gamma\cdot(p_1+p_1'))_2 , \\
P_2{}^N &= (i\gamma\cdot p_2)_1\,(1)_2 ,
\end{aligned}
\tag{A11}
$$

and

$$
P_2{}^P = (1)_1\,(i\gamma\cdot p_1)_2 ,
$$

so that

$$P_2 = P_2{}^N + P_2{}^P.$$

Now G is reduced according to the expression given in the text

$$\begin{aligned} -(i\gamma_5\gamma_\mu)_1 (i\gamma_5\gamma_\mu)_2 = {} & m^2 \left[\frac{(s-u)^2}{stu}\right] P_1 - m\left[\frac{u^2-s^2}{stu}\right] P_2 \\ & + \left[\frac{(s+u)^2}{stu}\right] P_3 - m^2\left[\frac{4}{t}\right] P_5 \\ & + \left[\frac{u-s}{us}\right] G. \end{aligned} \tag{A12}$$

The remaining case is now

$$\begin{aligned} (\gamma_\mu i\gamma\cdot p_2)_1 (\gamma_\mu)_2 = {} & m\left[\frac{u-s}{su}\right] P_3 + \left[\frac{us - m^2(u+s)}{su}\right] P_2{}^P \\ & - m^2\left[\frac{u+s}{su}\right] P_2{}^N - m\left[\frac{su - m^2(u-s)}{su}\right] P_1 \\ & + m\left[\frac{t}{su}\right] G - Q_1 . \end{aligned} \tag{A13}$$

The result for the symmetric case is

$$\begin{aligned} (\gamma_\mu)_1 (\gamma_\mu i\gamma\cdot p_1)_2 = {} & m\left[\frac{u-s}{su}\right] P_3 + \left[\frac{us - m^2(u-s)}{su}\right] P_2{}^N \\ & - m^2\left[\frac{u+s}{su}\right] P_2{}^P - m\left[\frac{su - m^2(u-s)}{su}\right] P_1 \\ & + m\left[\frac{t}{su}\right] G - Q_2 . \end{aligned} \tag{A14}$$

REFERENCES

1. For a summary, see G. A. BAKER, JR., "Advances in Theoretical Physics," (K. A. Brueckner, Ed.), Vol. 1, Academic Press, New York, 1965.
2. P. CZIFFRA, M. H. MACGREGOR, M. J. MORAVCSIK, AND H. P. STAPP, *Phys. Rev.* **114** (1959), 881.
3. LOEFFEL, MARTIN, SIMON, AND WIGHTMAN, *Phys. Lett. B* **30** (1969), 656.
4. SANDRO GRAFFI, Stieltjes Summability and Convergence of the Padé Approximants for the Vacuum Polarization by an External Field, NYU Technical Report Number 25/71.
5. D. BESSIS AND M. PUSTERLA, *Nuovo Cimento A* **54** (1968), 243.

6. W. R. WORTMAN *in* "The Padé Approximant in Theoretical Physics," (J. L. Gammel and G. A. Brueckner, Jr., Eds.) Chapt. 14, Academic Press, New York, 1971.
7. D. BESSIS AND M. PUSTERLA, *Nuovo Cimento A* **54** (1968), 243.
8. J. A. CAMPBELL AND A. C. HEARNE, *J. Computational Phys.* **5** (1970), 280.
9. M. M. LÉVY, *Phys. Rev.*, **88** (1952), 725.
10. M. RUDERMAN, *Phys. Rev.* **90** (1953), 183.
11. A. KLEIN, *Phys. Rev.* **90** (1953), 1101.
12. G. BREIT, M. H. HULL, JR., K. E. LASSILA, AND K. D. PRATT, JR., *Phys. Rev.* **120** (1960), 2227.
13. W. R. WORTMAN, *Phys. Rev.* **176** (1969), 1762.
14. J. S. R. CHISOLM, *Proc. Cambridge Phil. Soc.* **48** (1952), 300.
15. D. AMATI, E. LEADER, AND B. VITALE, *Nuovo Cimento* **17** (1960), 69.
16. M. L. GOLDBERGER, M. T. GRISARU, S. W. MACDOWELL, AND D. Y. WONG, *Phys. Rev.* **120** (1960), 2250.
17. R. L. ANDERSON, S. N. GUPTA, AND J. HUSCHILT, *Phys. Rev.* **127** (1962), 1377.
18. J. L. GAMMEL, M. T. MENZEL, AND W. R. WORTMAN, *Phys. Rev. D* **3** (1971), 2175.
19. A. SCOTTI AND D. Y. WONG, *Phys. Rev.* **138** (1965), B145.
20. We thank a referee of *Phys. Rev.* for noting that we should emphasize this remark. We are presently engaged in applying this method to the graph of Fig. 1(*f*) and other graphs.
21. S. MACHIDA AND K. SENBA, *Progr. Theor. Phys.* **13** (1955), 389.
22. N. HOSHIZAKI, S. OTUKI, W. WATARI, AND M. YONEZAWA, *Progr. Theoret. Phys.* **27** (1962), 1199.
23. S. SAWADA, T. VEDA, W. WATARI, AND M. YONEZAWA, *Progr. Theoret. Phys.* (*Kyoto*) **28** (1962), 991.
24. R. A. BRYAN AND B. L. SCOTT, *Phys. Rev.* **135** (1964), B434.
25. T. UEDA AND A. E. S. GREEN, *Phys. Rev.* **174** (1968), 1304.
26. M. H. PARTOVI AND E. L. LOMON, *Phys. Rev. D* **2** (1970), 1999.
27. We are indebted to a referee of *Phys. Rev.* for this remark and the reference to Henley and Ruderman [28].
28. HENLEY AND RUDERMAN, *Phys. Rev.* **92** (1953), 1036.